Review of Nanomaterials in Dentistry: Interactions with the Oral Microenvironment, Clinical Applications, Hazards, and Benefits

Alexandros Besinis,[*,†] Tracy De Peralta,[‡,§] Christopher J. Tredwin,[‡] and Richard D. Handy[†]

[†]School of Biomedical & Biological Sciences, University of Plymouth, Drake Circus, Plymouth PL4 8AA, U.K. and [‡]Plymouth University Peninsula Dental School, University of Plymouth, John Bull Building, Tamar Science Park, Plymouth PL6 8BU, U.K. [§]Present address: School of Dentistry, University of Michigan, Ann Arbor, Michigan 48109-1078, United States.

ABSTRACT Interest in the use of engineered nanomaterials (ENMs) as either nanomedicines or dental materials/devices in clinical dentistry is growing. This review aims to detail the ultrafine structure, chemical composition, and reactivity of dental tissues in the context of interactions with ENMs, including the saliva, pellicle layer, and oral biofilm; then describes the applications of ENMs in dentistry in context with beneficial clinical outcomes versus potential risks. The flow rate and quality of saliva are likely to influence the behavior of ENMs in the oral cavity, but how the protein corona formed on the ENMs will alter bioavailability, or interact with the structure and proteins of the pellicle layer, as well as microbes in the biofilm, remains unclear. The tooth enamel is a dense crystalline structure that is likely to act as a barrier to ENM penetration, but underlying dentinal tubules are not. Consequently, ENMs may be used to strengthen dentine or regenerate pulp tissue. ENMs have dental applications as antibacterials for infection control, as nanofillers to improve the mechanical and bioactive properties of restoration materials, and as novel coatings on dental implants. Dentifrices and some related personal care products are already available for oral health applications. Overall, the clinical benefits generally outweigh the hazards of using ENMs in the oral cavity, and the latter should not prevent the responsible innovation of nanotechnology in dentistry. However, the clinical safety regulations for dental materials have not been specifically updated for ENMs, and some guidance on occupational health for practitioners is also needed. Knowledge gaps for future research include the formation of protein corona in the oral cavity, ENM diffusion through clinically relevant biofilms, and mechanistic investigations on how ENMs strengthen the tooth structure.

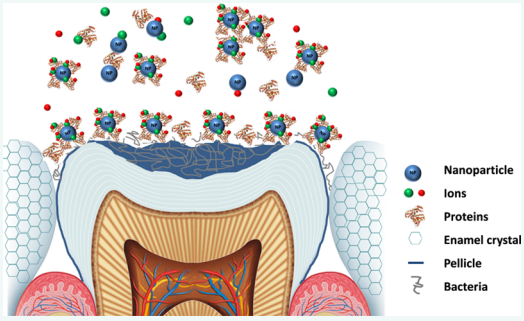

KEYWORDS: nanoparticles · protein corona · biomaterials · nanocomposites · dental implants · tooth chemistry · dentine · enamel · calcium hydroxyapatite · pulp stem cells differentiation · infection control · antibacterial activity

The medical applications of engineered nanomaterials (ENMs) are relatively well-known. These include antibacterial coatings for medical instruments and wound dressings (*e.g.*, self-sterilizing TiO_2 catheters;[1] nano-ZnO composite bandages[2]), the use of nanoencapsulation technology for improved drug delivery,[3,4] as well as exploiting the optical properties of nanomaterials for enhanced medical imaging.[5] Some of the clinical aspects above (*e.g.*, antibacterial ENMs) are particularly relevant to the oral cavity, and the role of ENMs in the control of the oral biofilm has been recognized.[6] Although the use of ENMs in dental applications has received some commentary,[7,8] a detailed evidence-based review has not been conducted, even though the use of nanotechnology in dentistry and dental materials has been the epicenter of extensive research in recent years.

In the oral cavity, nonclinical or occupational exposures are dependent on the use of nanoparticles (NPs) in food[9,10] and personal care products, such as dentifrices.[11] TiO_2 NPs are the most commonly used in food and personal care products (also known as E171 in food products, with 36% of the particles <100 nm[12]). The ingestion of TiO_2 via food is estimated to be relatively high (5 mg of TiO_2/person/d);[13] half of

* Address correspondence to alexander.besinis@plymouth.ac.uk, abessinis@hotmail.com.

Received for review September 5, 2014 and accepted January 27, 2015.

Published online January 27, 2015
10.1021/nn505015e

© 2015 American Chemical Society

which is in nanoparticulate form.[14] Numerous studies have investigated the potential toxicity of ENMs,[15,16] but the data is sparse on cells relevant to the oral cavity; although there is interest in using engineered and naturally occurring NMs to manipulate the cells/tissues associated with dentition (*e.g.*, controlling differentiation of pulp stem cells[17]). Some oral exposures have been done with rodents *in vivo*,[18,19] but none of these have collected samples to investigate potential pathologies in the oral cavity. Such data will be important in quantifying the risks of ENMs in the oral cavity and in supporting the notion of responsible and safe innovation of nanotechnology in dentistry.

As with any new medicine or medical device, the potential benefits must be weighed against the risks.[20,21] In terms of adverse health effects, there is a historic literature on the occupational exposure to dusts containing ultrafine particles[22] and the concern of respiratory toxicity from inhaling ENMs has also been reviewed for different ENMs (CNTs;[23,24] metal particles and silica[25]), with a particular focus on high aspect ratio ENMs that may cause acute inflammation in the lungs.[26] However, most of this literature has been concerned with events in the lung, not the oral cavity, and traditionally these experiments have used free forms of ENMs in aerosols or instillations, not ENMs that are embedded in the matrix of a commercial product, in semisolid materials like food, or in a dental material.

This review illustrates the evidence base for the applications of ENMs in dentistry. The electronic search was conducted applying a combination of subject terms and keywords on PubMed, Medline, Scopus, and Web of Knowledge databases. The electronic search terms focused on the four main application fields in dentistry (as antimicrobial agents, fillers in dental composites, dental implants, and in personal care products for the oral cavity), as well as the potential *in vivo* toxicity caused by ENMs following oral exposure. The keywords applied to the search databases were: (nanomaterial OR nanoparticle OR nanocoating OR nanotechnology) AND (antimicrobial OR antibacterial OR infection OR biofilm OR filler OR composite OR implant OR dentine OR enamel OR demineralization OR remineralization OR dentifrice OR toothpaste OR mouthwash OR oral product OR *in vivo* oral exposure toxicity) AND (dentistry OR dental OR oral). Quality criteria included considerations of experimental design in the published literature such as the use of appropriate bulk material or metal salt controls, and inclusion of information on at least the characterization of the starting material such as chemical composition, primary particle size, and size distribution where relevant. Papers with inadequate material characterization or poor descriptions of methodology or replication were excluded. The examples were also chosen to show a representative selection of materials, applications, and the historical chronology of the development of ENMs in this field. Selected examples from the published literature are presented in Tables 1−5.

VOCABULARY: **Engineered nanomaterials**-any intentionally manufactured material containing particles in an unbound state, or as an aggregate or as an agglomerate and where, for 50% or more of the particles in the number size distribution, one or more external dimensions is in the size range 1 to 100 nm; **Protein corona**-a dynamic layer of proteins and other biomolecules that spontaneously adsorb onto the surface of a nanoparticle, when the nanoparticle enters a biological fluid. The biological identity of the nanoparticle is then determined by this adsorption layer once the protein corona is formed. The biophysical properties of the nanoparticle−protein corona complex can very significantly compared to the nanoparticle alone, with consequent effects on the biological responses of cells or organisms; **Adsorption**-the process of biomolecule and/or solute accumulation at a cell membrane surface. Adsorption can be physical or chemical in origin. The biomolecular interactions of adsorption are governed by van der Waals forces, electrostatic attraction, and/or hydrogen bonding depending on the substances and surfaces involved; **Nanoparticle dissolution**-the dynamic process by which atoms or molecules from the surface of a nanoparticle go into the solution phase; such that the dispersion contains a homogeneous mixture of particles and dissolved solutes derived from the surface of the particle. The degree of dissolution is dictated by the solubility of the material and the available surface area for dissolution, in addition to traditional factors in solution chemistry such as temperature, pH, and ionic strength. As for any material, it is a prerequisite that the constituent molecules must be soluble to some degree in the local environment in order for a nanoparticle to dissolve; **Enamel**-the superficial layer that covers the crown of the tooth and is the hardest and most highly mineralized tissue in the body (96% w/w). The high mineral content renders enamel very strong, but also accounts for its brittleness. Enamel apatite consists of calcium hydroxyapatite and is highly crystalline with most crystals to be hexagonal; **Dentine**-a hydrated composite mineralized tissue that underlies enamel and forms the bulk of the tooth. Dentine is 70% inorganic, 20% organic, and 10% water by weight. The mineral phase is hydroxyapatite, similar to enamel, but dentine crystals have lower calcium content and are much smaller. The organic component of dentine is mainly collagen and is a permeable tissue due to the presence of the dentinal tubules; **Dental material**-a substance or combination of substances specially prepared and/or presented for use by authorized persons in the practice of dentistry and/or its associated procedures

The aims of this review were to (i) reflect on the ultrafine structure, chemical composition, and reactivity of teeth in the context of interactions with ENMs,

TABLE 1. Use of Antimicrobial Engineered Nanomaterials in Dental Materials[a]

nanomaterial characteristics	aim of application	treatment	key results	author
Chitosan (CS) functionalized with rose-bengal (RB) NPs were synthesized from CS NPs that were chemically cross-linked to RB using *N*-ethyl-N′-(3-dimethyl aminopropyl) carbodiimide (EDC 5 mM) and *N*-hydroxysuccinimide (NHS 5 mM). The particle size of the resulting CSRB NPs was 60 ± 20 nm.	To introduce an antibiofilm effect and stabilize the structural-integrity of dental root dentine by photo-cross-linking dentine collagen matrix.	An *E. faecalis* biofilm was left to mature for 21 days before being challenged with CSRB NPs (0.1 and 0.3 mg mL^{-1}) or RB (10 μM) for 15 min and exposed to photodynamic therapy (dosage of 20, 40, and 60 J cm^{-2}; and fractionated dosage of 10 and 20 J cm^{-2} twice). The cytotoxicity tests were performed using mouse fibroblast cells. Incubation time after exposure was 15 min in the dark. CSRB NPs and RB were tested with radiation (20 J cm^{-2}) and without radiation.	Complete death of biofilm bacteria was not achieved with either CSRB or RB even at 60 J cm^{-2}. The best antibacterial effect was achieved with fractionation of the dosage (20 + 20 J cm^{-2}) with complete elimination of biofilm bacteria in the case of 0.3 mg mL^{-1} CSRB NPs. The initial thickness of the biofilm was 39.2 ± 7.3 μm, which was reduced to 13.1 ± 4.3 and 23.1 ± 5.57 μm after CSRB NPs and RB treatment, respectively. CSRB NPs showed no dark toxicity (95.5 ± 12% cell survival), but toxicity was higher following irradiation (72.86 ± 9% cell survival).	Shrestha *et al.* (2014)[255]
50 nm ZnO NPs and 20 nm Ag NPs	Resin composite with antibacterial activity to inhibit the growth of oral cavity microorganisms.	ZnO or Ag NPs were added to a resin composite material at a concentration of 1 wt %. Disc-shaped specimens were prepared using light treatment. The antibacterial activity was tested against *S. mutans* and *Lactobacillus* after 12 h of incubation.	Measurement of the active colonies formed on the surface of blood agar plates showed a significant antibacterial activity for the resin composites with added ZnO NPs (0.93 ± 1.53 CFU for *S. mutans* and 1.20 ± 0.77 CFU for *Lactobacillus*) or added Ag NPs (7.33 ± 7.19 and 0.73 ± 0.79 CFU, respectively) compared to the control group (126.0 ± 29.47 and 3.80 ± 2.54 CFU, respectively).	Kasraei *et al.* (2014)[256]
2.7 nm Ag NPs. Ag NPs were synthesized by dissolving silver 2-ethylhexanoate powder in 2-(*tert*-butylamino)ethyl methacrylate (TBAEMA) at 0.1 g of silver salt per 0.9 g of TBAEMA.	An adhesive/primer system with improved antibacterial activity.	5% of aquaternary ammonium monomer (dimethylaminododecyl methacrylate, DMADDM) and 0.1% of Ag NPs were incorporated into a primer and an adhesive.	The agar plate diffusion test showed that primer specimens containing 0.1% Ag NPs had significantly larger inhibition zones compared to controls. The MTT assay and lactic acid production results showed that the metabolic activity of bacteria on specimens containing Ag NPs was significantly lower. The colony forming unit (CFU) value for the DMADDM + Ag NPs specimens was 10^7 compared to 0.4×10^9 for the controls without Ag NPs.	Cheng *et al.* (2013)[257]
Colloidal solution of lactose-modified chitosan (Chitlac)-Ag NPs. Ag NPs were obtained from $AgNO_3$ after mixing with ascorbic acid. Size of Chitlac-Ag NPs clusters was 1—5 μm.	Antimicrobial coating for medical devices and implants.	Thermoset surfaces were coated with 0.5 mM Chitlac-Ag NPs. Antibacterial activity was tested against *S. aureus* and *P. aeruginosa* (3 h). Cytotoxicity tests were performed using human skin fibroblasts and osteoblast-like cells (24—72 h).	Viability of bacteria after exposure to treated surfaces was 6 times less (1 log CFU mL^{-1}) compared to untreated surfaces (6 log CFU mL^{-1}). LDH release after 72 h contact with treated surfaces was 15% for fibroblasts (control was 21%) and 8% for osteoblast-like cells (control was 9%).	Travan *et al.* (2011)[140]
Quaternary ammonium polyethylenimine (QPEI) NPs were added in a resin composite containing 47% zirconia-silica particles with average size 0.01—6.0 μm. Size of QPEI NPs not given. Components were manually mixed for 20 s.	Resin composite with antibacterial activity.	Disc-shaped control composites and composites with 1 wt % QPEI NPs were placed intraorally in patients. Biofilm formation was allowed for 4 h before testing.	71% of bacteria remained viable on control resin composite compared to 19% on samples containing QPEI NPs. Incorporation of QPEI NPs increased the biofilm thickness to 107 μm (was 69 μm on control surfaces).	Beyth *et al.* (2010)[151]

Table 1. Continued

QPEI NPs were incorporated into a commercial provisional cement. Size of the NPs was not provided.	Provisional restorations with long-term antibacterial effect.	QPEI NPs were introduced to the restoration material at 0.5, 1, and 2 wt %. Microtiter plates were coated with the final product and the antibacterial effect of 24 h and 14 day aged samples was tested against *S. mutans* and *E. faecalis*.	No bacterial growth was observed for the 24 h aged samples. No growth of *S. mutans* was observed on samples aged for 14 days. No growth of *E. faecalis* was also observed on 14 day aged samples where the QPEI NPs concentration was higher than 1 wt %.	Shvero *et al.* (2010)[152]
Sol—gel derived bioactive glass nanopowders (58S, 63S, 72S). Particle size was 20—90 nm.	Orthopedic infection control and disinfection of root canal.	Bacteria (*E. coli*, *S. aureus*, *S. typhi*, *P. aeuginosa*) were cultured in broth containing bioactive glass NPs at different concentrations (6.25—100 mg mL^{-1}) for 24, 48, 72, 96, and 120 h. Cytotoxicity was assessed by the MTT assay using mouse fibroblasts.	The minimum bactericidal concentration (MBC) of 58S was 50 mg mL^{-1} against *E. coli* and *S. aureus* and 100 mg mL^{-1} for *S. typhi*, and *P. aeruginosa*. MBC of 63S was recorded at 100 mg mL^{-1} for *E. coli* and *S. aureus* but had no effect on *S. typhi* and *P. aeruginosa*. 72S showed no bacterial effect. At 72 h, 63S was not statistically different from the control, but 58S and 72S showed greater cell viability and proliferation.	Mortazavi *et al.* (2010)[150]
40—100 nm ZnO NPs and 30 nm TiO_2 NPs.	Resin composites with antimicrobial activity to prevent biofilm formation.	ZnO NPs were introduced to a microhybrid composite at 1, 5, and 10 wt %. Also 10% ZnO or TiO_2 NPs were added to a nanofilled composite. Antibacterial activity was tested against *S. sobrinus* after 3 days of biofilm formation.	Minimum inhibitory concentration (MIC) of ZnO NPs was 50 μg mL^{-1}, whereas the MBC was 150 μg mL^{-1}. There was a 20% reduction in biofilm growth on composite discs containing 10% ZnO. Antibacterial effect on discs with 10% TiO_2 was similar to controls.	Aydin and Hanley (2010)[143]
TiO_2 NPs (25—85 nm). Anatase to rutile phase was 3:1.	Dental adhesives with long-term bacteria inhibition properties.	TiO_2 NPs were added to a commercial dental adhesive at 5, 10, 20, and 30 wt %. The nanoadhesive was then spread on a 1.2 cm^2 disc and light cured. Samples were coated with *S. epidermidis* and UV irradiated for up to 120 min.	Bacteria harvested from the specimens containing 20% TiO_2 NPs produced 12 colonies per sample, while 10% containing samples only 1 colony. The incorporation of 20% TiO_2 NPs did not increase the tensile bond strength of specimens (18 N) compared to control.	Welch *et al.* (2010)[124]
Nanometric bioactive glass 45S5 prepared by flame spray synthesis (particle size was not given) and also micrometric 45S5 bioactive glass (particles <5 μm).	Root canal disinfectant.	Caries and restoration free human premolars were seeded with 0.1 mL of *E. faecalis*, and then root canals were filled with nano-45S5, micro-45S5, or a 50:50 mixture of both.	Nano-45S5 had a 12-fold higher surface area compared to its micrometric counterpart. All specimens treated with nano-45S5 showed bacterial growth (12 out of 12), while micro-45S5 was significantly more effective (1 out of 12). Three out of 12 specimens dressed with the nanomicro mixture showed bacterial growth.	Waltimo *et al.* (2009)[258]
Ag NPs (particle size <5 nm).	Composite adhesive with antibacterial activity to prevent enamel demineralization.	Ag NPs were added to the adhesive at 0, 250, and 500 ppm. Disc-shaped (3 × 2 mm) specimens were prepared, and their effect was determined on the bacterial growth on liquid media (incubation time up to 24 h at 37 °C) and with agar diffusion assay (incubation time 48 h at 37 °C). *S. mutans* and *S. sobrinus* were the bacterial strains tested.	After 24 h of incubation, the bacterial growth was measured spectrophotometrically (A_{660}) and the optical density values for specimens containing 0, 250, and 500 mg L^{-1} Ag NPs were 0.70 ± 0.07, 0.72 ± 0.06, and 0.69 ± 0.05, respectively, in the case of *S. mutans*. The corresponding values for *S. sobrinus* were 0.70 ± 0.05, 0.68 ± 0.10, and 0.71 ± 0.11. The values for blanks were 0.73 ± 0.07 (*S. mutans*) and 0.70 ± 0.05 (*S. sobrinus*). The agar diffusion assay showed no zones of inhibition.	Ahn *et al.* (2009)[137]

Table 1. Continued

Ag NPs (100−120 nm). An aqueous Ag sol was synthesized from a water solution of 10 mmol L^{-1} $AgNO_3$ and 2% PVP. The solution was deaerated with argon gas for 1 h and treated with 20 KGy ^{60}Co gamma-radiation.	Oral tissue conditioner with antimicrobial activity.	Disc samples of 20 × 3 mm of tissue conditioner containing Ag NPs at 0.1, 0.5, 1.0, 2.0, and 3.0% (vol/vol % Ag sol/conditioner liquid) were prepared. Specimens were placed in culture plates, and their antibacterial activity was tested against *S. mutans*, *C. albicans*, and *S. aureus* after 24 and 72 h of incubation at 37 °C.	An inhibitory effect was observed against all bacterial strains even for specimens with the lowest (0.1%) Ag content. For *S. mutans*, *C. albicans*, and *S. aureus*, no CFUs were observed for specimens containing 1, 2, and 1% Ag, respectively. There were no statistical differences between incubation times of 24 and 72 h.	Nam (2011)[139]
Ag NPs (particle size not specified).	As an antimicrobial coating for dental implants.	A TaN-Ag nanocomposite coating (1.4−1.7 μm thick) was synthesized by a twin-gun reactive magnetron sputtering and deposited on 50 mm of pure Ti plate specimens. The samples tested contained 0, 14.9, 17.5, and 21.4% Ag. Control Ti samples were uncoated. The antimicrobial efficacy of the specimens was evaluated using *S. aureus*. Samples were inoculated with bacteria and incubated for 6 h at 37 °C.	The highest relative fluorescence intensity of the bacterial retention was observed on the uncoated Ti surfaces (97 ± 3 arbitrary units) followed by TaN-Ag14.9% (92 ± 2), TaN-Ag17.5% (84 ± 4), TaN (69 ± 3), and TaN-Ag21.4% (57 ± 3). The *S. aureus* growth on uncoated Ti samples was 44 CFU cm^{-2} and 37 CFU cm^{-2} on TaN coated samples and 3 CFU cm^{-2} on TaN-Ag 21.4% coated samples.	Huang *et al.* (2010)[138]

[a] MTT, 3-(4,5-dimethylthiazol-2-yl)-2,5-diphenyltetrazolium bromide. Studies are presented in chronological order for convenience.

and to set the scene on the nanoscale biology and surface film events in the oral cavity, (ii) describe the main actual and proposed applications of ENMs in dentistry, and (iii) put the dental applications in context of clinical outcomes versus potential hazards as well as risks. Finally, (iv) key knowledge gaps are identified with some recommendations for future research.

PROPERTIES OF SALIVA AND THE BEHAVIOR OF ENMS

Saliva is a complex mucous secretion that functions to maintain the pH in the oral cavity, mostly via bicarbonate and some calcium phosphate buffering.[27] Acids derived from the consumption of food and drink and/or bacterial metabolism are neutralized by bicarbonate (Figure 1B) in order to prevent acid erosion of the teeth.[28,29] Additionally, saliva has a rinsing effect on teeth and contributes to bacteria clearance, but it also contains antibacterial proteins (*e.g.*, lysozyme, iron chelators such as lactoferrin) and components of the immune system (*e.g.*, immunoglobulins). Clearly, the antimicrobial properties of ENMs are of interest in relation to the latter functions (see below), but the behavior of ENMs in saliva will also be influenced by the pH, electrolyte composition, and viscous properties of the mucus components.

It is not our intention here to detail the complex physicochemistry of ENMs in biological media, but to appreciate the importance of the colloidal properties of ENMs that might be important for saliva. First with respect to colloid chemistry, most ENMs are not in true aqueous solution but are dispersed in the liquid phase; with the aggregation of the materials being particularly influenced by the ionic strength of the medium, the presence of divalent ions like calcium, pH, and the presence of organic matter.[30−33] Saliva is 99% water and is a high ionic strength medium containing numerous electrolytes. The exact electrolyte concentrations in saliva can vary, but it normally contains (in mmol L^{-1}); sodium (2−26), potassium (13−40), phosphate (2−22), calcium (0.5−2.8), chloride (8−40), iodide (2−22), bicarbonate (0.1−8), magnesium (0.15−0.6), and a trace amount of fluoride (usually at μmol L^{-1}). These concentrations may be higher in freshly stimulated saliva.[34] The millimolar concentrations of NaCl and the divalent ions such as Ca^{2+} and Mg^{2+} will tend to promote particle aggregation.[31] Consequently, similar to physiological salines,[35] saliva may promote the settling of aggregates of the ENM onto the surfaces of the oral cavity.

The resulting effects of ENMs in a dental material on the bulk electrolyte functions of saliva are likely to be modest since the millimolar concentrations of NaCl and Ca^{2+} in the saliva would (theoretically) be in excess of any labile ENM. For example, Besinis *et al.* found only negligible low micromolar release of silver from dentine slices coated with Ag NPs.[36] The rheology and viscous properties of mucous solutions are mainly

TABLE 2. Use of Engineered Nanomaterials as Fillers in Dental Composite Applications[a]

nanomaterial characteristics	aim of application	treatment	key results	author
Hybrid silica/acrylic NPs were synthesized by seeded emulsion polymerization. Following methyl methacrylate (MMA) polymerization, a poly(methyl methacrylate) (PMMA) shell (3—6 nm thick) was formed on the surface of silica NPs. Core NPs had a diameter size of 59.4 ± 14.4 nm, whereas hybrid NPs were larger (silica/PMMA 78/22, D = 75.8 ± 12.5 nm; 57/43, D = 81.2 ± 15.4 nm).	As nanofillers to increase the silica filler content in dental resin composites.	The silica or hybrid (silica/PMMA at ratios of 78/22 and 57/43) NPs were introduced to the resin and were mixed manually until the powder was completely wetted. The filler content in the specimens prepared was 20, 30, or 40 wt % for the silica NPs and 40, 50, or 60 wt % for the hybrid NPs.	Composites containing 30 wt % silica NPs demonstrated the highest flexular strength (57 MPa), which decreased with further increase of the filler content (48 MPa for 40 wt %). The flexular strength of composites prepared with hybrid NPs at the same filler content (40 wt %) was considerably lower (25 MPa for the 78/22 NPs and 30 MPa for the 57/43 NPs). The flexular modulus of composites containing 40 wt % silica NPs was 3091 MPa and the respective value for composites carrying hybrid 78/22 NPs at the same filler content was 2694 MPa. The flexular modulus for composites with filler particles carrying a higher amount of PMMA (57/43) was significantly lower (1528 MPa). The use of hybrid NPs enabled the incorporation of a higher concentration of silica in the composites and better dispersion of the filler particles.	Canché-Escamilla *et al.* (2014)[259]
HA NPs (20—70 nm) were prepared following biomimetic and hydrothermal processes.	As nanofillers to reinforce an adhesive system.	HA NPs were incorporated into the resin solutions of the adhesive system at 0.2%, 1%, 5%, and 10% (w/v). Fillers were mechanically stirred with the resins and sonicated for 30 min to ensure dispersion.	The control group had a mean microtensile bond strength (μTBS) of 52.1 ± 16.6 MPa, which increased significantly for the adhesive containing 1% of the biomimetic HA NPs (59.5 ± 11.9 MPa). The μTBS for 10% filler content was significantly lower for all types of HA NPs ranging from 33 to 42 MPa.	Wagner *et al.* (2013)[260]
Zirconia NPs (20—50 nm) were prepared by laser vaporization.	As nanofiller to improve the properties of resin/adhesive.	Zirconia NPs were incorporated into the primer or adhesive of a commercial adhesive system at different concentrations (5, 10, 15, and 20 wt %). Mixtures were sonicated for 1 h to increase dispersion prior to application.	Incorporation of zirconia NPs at 20 wt % in the primer increased the μTBS to 41 ± 13 MPa. When added at the same concentration to the adhesive, μTBS was 32 ± 15 MPa. μTBS for control was 25 ± 11 MPa.	Lohbauer *et al.* (2010)[168]
CaF_2 NPs (56 nm) were synthesized by spray-drying.	Resin composite with improved mechanical properties and fluoride release.	CaF_2 NPs were incorporated in a glass-reinforced composite at 10, 20, and 30 wt %. Specimens were immersed in a NaCl solution and monitored up to 84 days.	The flexular strength of nanocomposites containing 10, 20, and 30% CaF_2 was 170 ± 20, 125 ± 15, and 100 ± 15 MPa, respectively, before immersion. After 84 days of immersion (pH 4) the corresponding values were 130 ± 15, 117 ± 10, and 70 ± 10 MPa. At 84 days, the fluoride release was 47, 252, and 327 μg cm^{-2}, respectively.	Xu *et al.* (2010)[170]

Table 2. Continued

HA nanorods were synthesized by hydrothermal method. Particle size was not given.	As nanofillers to improve the properties of dental adhesives.	HA nanorods were added to an experimental ethanol based adhesive at 0.2—5 wt % and sonicated for 1 min.	Diametral tensile strength was higher when 0.2 and 0.5 wt % HA had been incorporated (35 ± 5 and 33 ± 2 MPa compared to 25 ± 5 MPa for control). The highest flexular strength was observed at the same filler contents and was 50 ± 5 and 52 ± 5 MPa, respectively (41 ± 8.1 MPa for control). Specimens with 0.2% HA had the highest microshear bond strength (22 ± 3 MPa compared to 11 ± 3 MPa for control). Flexular strength remained unchanged.	Sadat-Shojai *et al.* (2010)[171]
Silica NPs (20—50 nm, mean diameter 26 nm) and 10—40 μm silica microparticles (mean diameter 18 μm). Silica NPs were treated with γ-methacryloxypropyltrimethoxysilane (γ-MPS) and left to dry for 20 days.	As nanofillers to improve mechanical properties of dental resin composites.	25 × 2 × 2 mm specimens were prepared. Specimens contained 20, 30, 40, and 50 wt % silica NPs or 60 wt % microsilica (control).	Composites containing 40 wt % silica NPs demonstrated the highest fracture toughness and flexular strength (1.4 ± 0.1 MPa $m^{1/2}$ and 149.7 ± 8.1 MPa, respectively). 50 % filler content had the highest Vickers hardness (70.1 ± 3.7 VHN). Composites containing 60% microsilica had similar properties with those containing 20% silica NPs.	Hosseinalipour *et al.* (2010)[172]
1 nm thick and up to 1 μm long and wide sodium montmorillonite (Na-MMT) plate-like particles.	As nanofillers to increase the bond strength of dentine bonding systems.	Na-MMT particles were modified by methyl methacrylate by graft polymerization. The modified NPs were incorporated into an adhesive at 0.2, 0.5, 1, 2, and 5 wt %. Fillers were dispersed by sonication. The adhesive was applied to 3 mm thick human dentine discs etched with 35% phosphoric acid for 15 s.	The adhesive containing 0.5 wt % PMMA-modified Na-MMT NPs had the highest microshear bond strength (30 ± 7 MPa). The corresponding values for adhesives with filler content 0, 2, 1, 2, and 5 wt % were 26 ± 5, 24 ± 10, 24 ± 5, and 19 ± 6 MPa. The value for the control was 20 ± 6 MPa.	Atai *et al.* (2009)[169]
ZrO_2—SiO_2 NPs were synthesized according to a sol—gel technique. Primer NPs were 50 nm and agglomerates up to 10 μm.	As nanofillers to improve the properties of resin-based restorative materials.	The restorative material contained nanofiller (23% ZrO_2/72% SiO_2) at 74%. 25 × 2 × 2 mm specimens were prepared. Specimens containing glass microparticles at the same concentration were also made and used for comparison. Flexular strength was measured after specimens were stored in water at 37 °C for 24 h and also after being stored at 37 °C for 4 weeks and then thermocycled 5000 times between water baths at 5 and 55 °C.	Flexular strength of the specimens containing NPs was 68 ± 11 MPa compared to 93 ± 8 MPa for specimens with glass micropartides. After thermocycling, flexular strength was 42 ± 6 and 66 ± 8 MPa, respectively. Both materials showed the same solubility (1.48 ± 0.04 μg mm^{-3}) and similar shrinkage (3.5 ± 0.3 and 3.0 ± 0.5 vol %, respectively). Water sorption (82 ± 2.6 μg mm^{-3}) and X-ray opacity (27 ± 2.9 mm) of the nanofilled material was significantly higher compared to its micro counterpart (30 ± 6.3 μg mm^{-3} and 7 ± 1.1 mm).	Ruttermann *et al.* (2008)[174]
Spherical monodisperse SiO_2-based Ta_2O_5 NPs were synthesized by flame-spray pyrolysis (primary particle size was 10 nm).	Radiopaque dental adhesive.	The particle surface was functionalized with γ-MPS in cyclohexane at 70 °C for 24 h. The particles were manually mixed with the dental adhesive matrix and then dispersed by ultrasonication. The filler content was 1 and 20 wt %. The Ta_2O_5 weight fraction in the final powder product ranged between 35 and 83 wt %. Dental adhesive was applied to enamel and dentine of bovine incisors previously etched with 37% phosphoric acid gel.	The method of dispersion (centrifugal mixing, sonication, or both) was found to affect the sedimentation of the particles. Centrifugal mixing along with ultrasonication gave the best results with 86% of the particles being <30 nm. Samples with 35 wt % Ta_2O_5 had lower radiopacity than dentine (72% Al), while samples with 83 wt % Ta_2O_5 had higher radiopacity than dentine and enamel (170% Al). Unfilled adhesive demonstrated the strongest adhesion on dentine (16.1 ± 4.0 MPa), while adhesive with 20 wt % functionalized filler content was most effective on enamel (26.8 ± 5.1 MPa).	Schulz *et al.* (2008)[178]

Table 2. Continued

Single-walled carbon nanotubes (SWCNTs) with a diameter of <10 nm and mean length of 15 μm.	Resin-based composite with improved mechanical properties.	SWCNTs were oxidized with H_2SO_4 and HNO_3 for 8 h under ultrasonication and rinsed with ethanol. SWCNTs were nanocoated with SiO_2 by a hydrolysation process. 25 $\times$ 2 $\times$ 2 mm composite specimens were prepared containing 0.1 wt % SiO_2—modified SWCNTs.	The flexular strength of SWCNTs specimens was 141.1 $\pm$ 8.4 MPa compared to 115.0 $\pm$ 3.2 MPa for the unfilled controls.	Zhang *et al*. (2008)[175]
Silica NPs. The particles used were 7 and 40 nm in diameter and had a surface area of 50 and 380 $m^2\ g^{-1}$, respectively. NPs were treated with γ-MPS.	Nanocomposites with improved aesthetic properties.	1 mm thick composites were prepared. Resin matrix was loaded with 70 wt % microfillers (Ba-glass, 1 μm) and 6 wt % of different combinations of 7 and 40 nm silica NPs.	The contrast ratio of the specimens was found to decrease with increasing content in 7 nm silica NPs. Specimens containing 6 wt % 7 nm silica NPs exhibited the lowest contrast ratio (0.51 $\pm$ 0.03 at 400 nm). Translucency was reduced with increasing concentration in 40 nm silica NPs. The lowest translucency was measured for specimens containing 5 wt % 40 nm NPs and 1 wt % 7 nm NPs (0.78 $\pm$ 0.02).	Kim *et al*. (2007)[177]
$BaSO_4$ NPs. Particle size was <10 nm.	To control the reaction time and mechanical properties of glass ionomer cements.	A glass ionomer powder was manually mixed with 1, 2, 5, 10, 15, and 25 wt % $BaSO_4$ NPs. Six mm in height and 4 mm in diameter cylindrical specimens were prepared in molds.	Increasing concentration in $BaSO_4$ NPs initially resulted in reduced working times and initial setting times, but for higher concentration the effect was reversed. The shortest working time was for specimens with 5 wt % $BaSO_4$ NPs (132.4 $\pm$ 9.5 s) and the shortest initial setting time for 15 wt % particle content (338 $\pm$ 10.4 s). The corresponding values for the controls were 155.4 $\pm$ 15.1 and 442 $\pm$ 32.7 s. Incorporation of NPs in the glass cement decreased the compressive strength even at low concentrations. Compressive strength for samples containing 1% $BaSO_4$ was 142 MPa compared to 160 MPa for the control. Samples with nanoparticle concentrations >10% had reduced surface hardness too.	Prentice *et al*. (2006)[173]
Ytterbium fluoride (YbF_3) NPs, 25 nm.	To control the reaction time and mechanical properties of glass ionomer cements.	YbF_3 NPs were incorporated in a glass ionomer cement at 1, 2, 5, 10, 15, and 25 wt %. Compressive strength and surface hardness tests were performed using 6 $\times$ 4 mm cylindrical specimens.	Glass cement specimens with an increasing content in YbF_3 NPs demonstrated shorter working and initial setting times. The corresponding values for specimens containing 25 wt % YbF_3 NPs were 44.0 $\pm$ 2.9 and 145.0 $\pm$ 6.1 s compared to 155.4 $\pm$ 15.1 and 442 $\pm$ 32.7 s for the controls. The compressive strength of the control was 160 MPa. Addition of NPs at 5 and 25 wt % reduced the strength values at 145 and 105 MPa, respectively. Incorporation of NPs up to 5 wt % increased the surface hardness of the specimens to 43 VHN from 40 VHN but higher concentrations reduced the surface hardness (29 VHN for 25 wt % NP content).	Prentice *et al*. (2006)[173]

[a] Studies are presented in chronological order for convenience.

TABLE 3. Use of Engineered Nanomaterials in Dental Implant Applications[a]

nanomaterial characteristics	aim of application	treatment	key results	author
Copper (Cu) decorated multiwalled carbon nanotubes (MWCNTs) were produced following the wet chemical method and using copper acetate as a precursor. The inside and outside diameters of the MWCNTs were 10—20 and 40—60 nm, respectively. The length of MWCNTs was 2—10 μm. The size of Cu, Cu_2O, and CuO crystallites was 4.6, 10, and 13 nm, respectively.	As a biocompatible nanocoating on Ti-6Al-4V dental implants to improve the microstructural and nanomechanical properties of fluorapatite (FA)-based composite coatings.	FA-TiO_2-MWCNT-Cu nanotubes were synthesized following the sol—gel technique and applied to Ti-6Al-4V specimens following a spin coating process. All Ti alloy specimens (10 mm $\times$ 10 mm $\times$ 1 mm) had been previously polished to remove original oxides and surface defects.	The indentation depth for the different nanocoatings tested was FA > FA-TiO_2-MWCNT-Cu > FA-TiO_2. Addition of 10 wt % TiO_2 and 1 wt % MWCNT-Cu was found to increase the elastic modulus of FA up to 60%. The elastic modulus of the FA, FA-TiO_2, and FA-TiO_2-MWCNT-Cu coatings was 11.8, 14.5, and 19.3 GPa, respectively. The FA-TiO_2 composite coating demonstrated the highest Vickers hardness (0.72) followed by the FA-TiO_2-MWCNT-Cu (0.58) and FA (0.37) coatings.	Sasani *et al.* (2014)[261]
HA NPs (70—80 nm) were produced according to an electrochemical deposition method, where $Ca(NO_3)_2$ and $NH_4H_2PO_4$ were dissolved in distilled water to a Ca/P ratio of 1.67.	As a coating on titanium implants to improve osteoblast cell proliferation and differentiation.	Titanium plates of 10 $\times$ 10 $\times$ 1 mm were polished, sandblasted, and washed in 75% acetone in an ultrasonic bath. Before applying the nano-HA coatings, specimens were treated with a solution containing HF and HNO_3 and a second solution containing HCl and H_2SO_4. Murine preosteoblast cells (MC3T3-E1) were seeded at a density of 1 $\times$ 10^5 on each plate and cultured up to 21 days.	The protein content of cells growing on nano-HA coated plates (14 μg plate^{-1}) was significantly higher compared to the control group (5 μg plate^{-1}) at early stage (day 7). The alkaline phosphatase (ALP) activity (0.5 nmol μg^{-1} h^{-1}) and octeocalcin production (1 ng μg^{-1} protein) of cells in the nano-HA group were significantly higher compared to the uncoated control group (0.4 nmol $\mu g^{-1} h^{-1}$ and 0.75 ng μg^{-1} protein, respectively) after 21 days of culture.	Shi *et al.* (2013)[262]
Carbon nanotubes (CNTs) synthesized by a chemical vapor deposition. Size was not specified.	Biodegradable bioactive polymer-based material to be used in bone fixatives for maxillofacial surgery applications.	CNTs were dissolved in tetrahydrofuran solvent and mixed with calcium phosphate (CP) and poly(lactic acid) (PLA). The final composites (PLA-CPNT1 and PLA-CPNT2) contained 0.1 and 0.25 wt % CNTs. Disc-shaped specimens (1 $\times$ 10 mm) were prepared in molds at 180 °C. 4 $\times$ 10^4 preosteoblast cells were seeded on each sample and cultured for 14 days. Cell viability was measured by the MTS method and the cell differentiation into osteoblasts by the ALP activity.	The highest tensile strength was measured for PLA samples consisting of 50% CP and 0.25% CNTs (15.9 $\pm$ 0.9 MPa) when compared to PLA controls (6.0 $\pm$ 0.9 MPa). During the 14 day culture period there was an increase in cell growth (apart from a drop observed after 7 days for PLA-CPNT2 samples). After 14 days, the cell growth on PLA, PLA-CPNT1, and PLA-CPNT2 samples was 1.75 $\pm$ 0.25, 2.10 $\pm$ 0.20, and 2.15 $\pm$ 0.10, respectively. The corresponding values for the ALP activity were 0.16 $\pm$ 0.01, 0.21 $\pm$ 0.03 and 0.17 $\pm$ 0.03.	Lee *et al.* (2011)[263]
HA nanocrystals (5 nm).	As a dental implant coating.	Screw-shaped titanium dental implants were either single or double coated with nano-HA. Specimens had been sandblasted and acid etched prior to coating. Implants were surgically placed in the tibia of New Zealand rabbits and removed after 2, 4, and 9 weeks of healing.	The thickness of the single coating was 20 nm, and of the double 40 nm. Interferometry results showed that the double coated implant had the smoothest surface (0.77 μm) and the uncoated control the roughest (1.08 μm). After 9 weeks of healing, the removal torque values for the control, single coated and double coated samples were 42 $\pm$ 10, 52 $\pm$ 10, and 48 $\pm$ 14 N cm, respectively. The corresponding values for the formation of new bone were 58 $\pm$ 6, 60 $\pm$ 9 and 59 $\pm$ 13%.	Svanborg *et al.* (2011)[191]

Table 3. Continued

CaP NPs (20—100 nm).	As a coating on maxillofacial implants to improve the peri-implant endosseous healing properties.	Implants with CaP modified surface NPs were surgically placed to 15 patients and removed 3 months later.	The bone area and the bone-to-implant contact (BIC) of the CaP modified implants were 9.1 and 13.3%, respectively, while the corresponding values for the control implants were 8.7 and 10.8%.	Telleman *et al.* (2010)[195]
CaP NPs. Particle size was not specified.	To modify the bone implant surfaces.	Titanium implants (5 mm in diameter and 11.5 mm long) were either alumina-blasted and dual acid-etched (controls) or impregnated with low levels of Ca (0.5%) and P (4%). Specimens were submerged into a suspension of either sarcoma osteogenic cells or mesenchymal stem cells and incubated at 37 °C up to 9 days. The cell adhesion on the implants was evaluated and also the cell behavior by ALP and MTT assays.	The average profile roughness of the control implants was 1.11 ± 0.30 and 0.84 ± 0.17 μm for those impregnated with CaP. Both cell types demonstrated an increasing proliferative activity over the 9 days of contact with the specimens. After 9 days of incubation, the MTT results for osteoblasts in contact with the controls were 0.32 ± 0.01 and 0.36 ± 0.01 AU for cells in contact with the CaP modified specimens. The respective values for mesenchymal cells were 0.15 ± 0.01 and 0.13 ± 0.01 AU. There was a reduction in the ALP activity of osteoblasts and mesenchymal cells in contact with both control and modified samples after 6 days.	Bucci-Sabattini *et al.* (2010)[196]
HA NPs (1—150 nm), suspended in a toluene-based solution were used to coat Ti (cpTi) and titanium alloy (Ti-6Al-4V) implants by discrete crystalline deposition.	To modify the surface of titanium implants and promote osseointegration.	Nano-HA modified cylindrical (2 × 1 mm) implants were placed in the femur of 8-week-old rats. Implants were harvested after 4 days, 1 week, and 2 weeks for examination.	Up to 1 week, healing results for modified and unmodified implants were similar. However, after 2 weeks the push-in value for the nano-HA coated cpTi implants was significantly higher (32 N) compared to untreated implants (20 N). For the Ti-6Al-4V implants, the push-in values were 40 and 26 N, respectively. The mean BIC for the coated and uncoated specimens was 61 ± 7 and 56 ± 11%, respectively.	Lin *et al.* (2009)[188]
Rod-like nano-HA crystals. The cross-sectional diameter of the HA nanorods was 70—80 nm.	As a coating on porous titanium implants to promote osseointegration.	Screw-shaped titanium implants (8 mm long, 3 mm in diameter) were coated with nano-HA by an electrochemical deposition technique (3.0 V, 2 h at 85 °C). Implants were surgically placed in the proximal tibias of rabbits and harvested at 6 and 12 weeks following the operation.	At 6 and 12 weeks, the mean BIC for the coated implants was 30 ± 5% and 35 ± 10%, respectively (20 ± 2% and 31 ± 5% for the controls). At 12 weeks, the bone percentage within the threads inside the cortical bone was 85 ± 10% for the implants coated with nano-HA and 82 ± 5% for the uncoated specimens.	Yang *et al.* (2009)[189]
Rod-shaped HA NPs (particle size was not specified) coated pure titanium screw-shaped implants following an electrochemical deposition technique. The thickness of the HA coating was 1—2 μm.	As a coating for metallic implants to enhance bone bonding, osseointegration, and accelerate healing.	Titanium implants (10 mm long, 3 mm in diameter) were sandblasted, dual acid-etched, and heat treated with hydrogen peroxide before being electrochemically coated with nano-HA. Then implants were inserted into rabbit trabecular bone for 2—12 weeks.	Mean removal torque values for control samples harvested at 2, 4, 6, 8, or 12 weeks were 21 ± 4, 24 ± 6, 50 ± 10, 42 ± 6, and 50 ± 14 N cm, respectively. The corresponding values for coated specimens were 40 ± 15, 40 ± 15, 50 ± 16, 40 ± 13, and 51 ± 8 N cm showing that surface modification with nano-HA accelerates bone bonding and healing. After 4 weeks, results were similar.	He *et al.* (2009)[190]

Table 3. Continued

Diamond NPs (1—50 nm).	As a coating for orthopedic implants to regulate bone growth.	Nanodiamond (ND) coatings were produced by microwave plasma enhanced chemical vapor deposition and deposited on silicon wafers in the presence of 5—25% hydrogen gas (ND5-ND25) at 800 °C for 2 h. Osteoblasts were seeded on specimens at a density of 3500 cells cm^{-2} and cultured for 4 h to assess adhesion rates and up to 5 days to evaluate cell proliferation.	ND5 and ND10 particles were 20—80 nm in diameter, while the size of ND15, ND20, and ND25 was considerably larger (0.2—2 μm). Osteoblast adhesion for control silicon specimens, ND coated samples, ND5, and ND10 was 480 $\pm$ 100, 180 $\pm$ 70, 300 $\pm$ 50, and 320 $\pm$ 70 cells cm^{-2}, respectively. For higher hydrogen concentrations (>15%) cell adhesion was less than 200 cells cm^{-2}. After 5 days of culture, there were 3800 $\pm$ 600 cells cm^{-2} on ND5 specimens and 2000 $\pm$ 400 cells cm^{-2} on ND20. Osteoblast proliferation on controls was 1000 $\pm$ 400 cells cm^{-2}.	Yang *et al.* (2009)[199]
CaP NPs (20—100 nm).	As a coating on titanium alloy implants to enhance bone formation and healing.	Titanium alloy implants (2 mm in diameter and 9.5 mm in length) that had been previously acid etched were bonded with CaP nanocrystals. Implants were placed in the posterior maxillae of patients and retrieved after 4 or 8 weeks.	The histomorphometric results showed that the BIC for the CaP coated samples was 44.5 $\pm$ 7.4% after 4 weeks of healing and 45.3 $\pm$ 22.4% after 8 weeks. The respective values for the uncoated implants were 15.5 $\pm$ 4.6% and 18.3 $\pm$ 12.9%. After 4 weeks, the bone volume for the coated and uncoated specimens was similar, but after 8 weeks it was 44.5 $\pm$ 7.4% for the CaP treated samples and 18.8 $\pm$ 10.3% for the controls.	Goene *et al.* (2007)[194]
Yttrium-stabilized zirconia (YSZ) NPs. Single particle size was 50 nm. Particles formed 0.6 μm clusters.	Bioactive durable coating for biomedical implants.	A composite bilayer coating of YSZ and 45S5 NPs was deposited on chemically etched Ti6Al4V discs with a surface area of 1.5 cm^2. The coating was synthesized by an electrophoretic deposition method followed by sintering of the coated samples at 900 °C for 2 h.	The produced bilayer consisted of a 5 μm thick YSZ layer and a 15 μm layer of 45S5-YSZ. The universal hardness value was 0.35 $\pm$ 0.09 GPa and the elastic modulus 16.13 $\pm$ 3.0 GPa.	Radice *et al.* (2007)[200]

[a] Studies are presented in chronological order for convenience.

TABLE 4. Use of Engineered Nanomaterials in Dental Personal Care Products and Proposed Dentifrice Applications[a]

nanomaterial characteristics	aim of application	treatment	key point results	author
Polyethylene-glycol coated maghemite NPs (PEG-MNPs) were synthesized according to the "graft-to" method. Particle size was <25 nm.	To treat dentine hypersensitivity.	Tooth specimens were demineralized in a citric acid and EDTA solution for 10 min and then sonicated for 30 min to remove the smear layer and open the dentinal tubules. Each specimen was immersed in 5 mL of water containing 100 mg PEG-MNPs for 30, 60, 90, or 120 min. An external magnetic field was applied in order to direct the NPs to move inside the tubules.	SEM and energy dispersive X-ray spectroscopy (EDS) examination showed that the majority of the dentinal tubules were occluded with NPs following treatment with the water solution containing PEG-MNPs. The exposure time was found to be important, and the best results were achieved for specimens treated for 120 min.	Dabbagh *et al.* (2014)[264]
Spherical silica NPs (12 nm) and HA NPs (3—5 nm). HA NPs were synthesized according to the sol—gel technique.	To encourage remineralization of fully demineralized dentine.	Fully demineralized dentine blocks (5 × 1 × 1 mm) were infiltrated with colloidal solutions containing silica and HA NPs for 24 h and then immersed in an artificial saliva for up to 12 weeks.	Infiltration of demineralized dentine with HA NPs for 24 h restored up to 55% of the P and Ca levels. Exposure of specimens infiltrated with silica NPs to artificial saliva resulted in a 20% restoration of the P levels and a 16% recovery of the mineral volume. The mineral separation after 4 weeks of remineralization was 18.7—20.6 μm for the silica NPs group compared to 15 μm for the sound control and 63.3—75.4 μm for the demineralized control.	Besinis *et al.* (2014)[104]
Mesoporous CaO silica (MCS) NPs (40 nm) were manufactured via a hydrothermal process.	As a paste to treat dentine hypersensitivity.	The MCS nanopaste was applied on 2 mm thick human dentine discs for 10 min before rinsing. Discs were pretreated with 17% EDTA for 5 min.	MCS NPs caused a nearly 100% occlusion of the dentinal tubules. The depth of penetration was 100 μm. MCS reduced dentine permeability. The fluid conductance was 13% (40% for the control desensitizer).	Chiang *et al.* (2010)[219]
Spherical silica NPs (40 nm)	As a dentifrice for dentine hypersensitivity.	1 mm thick dentine sections were polished, sonicated, and etched with 37 vol % phosphoric acid to remove the smear layer. Specimens were then infiltrated with 40 wt % silica NPs in water. Silica solutions were ultrasonicated for 5 min and then applied dropwise to dentine.	SEM examination showed that at least 50% of the dentinal tubules were significantly occluded.	Earl *et al.* (2009)[99]
Calcium carbonate NPs. Particle size was several tens to hundreds of nm.	As a dentifrice for the remineralization of enamel lesions.	Sections obtained from human sound molars were treated with a demineralizing solution to create subsurface lesions. Sections were then treated with a dentifrice containing 1% calcium carbonate (CC) twice a day for 4 weeks. During the rest of the day they were stored in artificial saliva at 37 °C.	Mineral loss for the baseline specimens (no remineralization) was 8.0 ± 2.2% × μm, for the specimens treated with a dentifrice containing 1% CC was 4.1 ± 1.2% × μm and for specimens treated with a non-CC dentifrice was 6.5 ± 2.0% × μm. Lesion depth was 184 ± 41, 148 ± 39, and 156 ± 40 μm, respectively. Maximum mineral density was 60.2 ± 14.9, 79.6 ± 8.1, and 66.3 ± 12.3%, respectively.	Nakashima *et al.* (2009)[215]
Calcium phosphate nanocrystals (<300 nm).	To promote dentine remineralization.	Dentine specimens were etched with phosphoric acid for 15 s and then immersed in a solution containing 500 mg mL^{-1} poly(acrylic acid), 200 mg mL^{-1} PVPA and 5 wt % Portland cement. Specimens were stored at 37 °C, and remineralization was allowed for up to 8 weeks.	The concentration of poly(acrylic acid) was found to regulate the formation of calcium phosphate nanocrystallites. Without poly(acrylic acid) the size of the crystals was 300 nm, while size was reduced at 75—100 nm in the presence of poly(acrylic acid) at 100 mg mL^{-1}. For concentrations >500 mg mL^{-1} poly(acrylic acid) behaved as an inhibitor and 50 nm calcium phosphate nanoprecursors were formed instead. Remineralization of the collagen matrix was observed after 6 weeks.	Tay and Pashley (2008)[100]
Carbonate hydroxyapatite (CHA) crystals (100 nm).	As a paste to cover defects on enamel surface and enhance remineralization.	Enamel slabs (3 × 3 mm) were brushed three times a day for 15 days with a CHA toothpaste using an electric toothbrush. Brushing sessions were for 30 s. Enamel specimens were washed with tap water after each session.	X-ray diffraction examination of the enamel surfaces treated with CHA toothpaste confirmed that CHA remained present even after brushing. SEM showed a thick homogeneous apatitic layer of CHA on enamel surfaces that filled any pits or scratches.	Roveri *et al.* (2008)[217]

Table 4. Continued

Spherical HA NPs (<100 nm) were synthesized by sintering at 700 °C. Also needle-like HA NPs (60 nm in length) were synthesized by precipitation.	As a paste to promote remineralization.	Solutions of spherical and needle-like HA NPs as well as a mixture of both types (particle size <2 μm) were added to a toothpaste without sodium fluoride. Specimens (human premolars with artificial caries) were treated for 5 and 10 days.	The hardness of demineralized enamel was 104 HV and that of sound enamel 287 HV. After 5 days of treatment with spherical HA NPs, needle-like HA, and mixed HA, the hardness of the specimens was 190, 200, and 150 HV, respectively. After 10 days of remineralization the corresponding values were 255, 260, and 175 HV.	Lv *et al*. (2007)[210]
45S5-type bioactive glass NPs were synthesized by flame spray synthesis. Particle size was in the range of 20—50 nm.	To increase the mineral content of dentine.	Dentine specimens previously demineralized with 17% EDTA for 2 h were immersed in suspensions of glass NPs or microglass at 37 °C for 1, 10, and 30 days.	In the slurry with nanoglass there was a rapid increase in the release of Ca^{2+} and dissolved silica. After 24 h the concentration values were 67.8 ± 3.7 and 22.3 ± 0.3 mg L^{-1}, respectively. Saturation levels had been reached within 6 h. Final ion concentrations for the slurry with microglass were 16.6 ± 2.6 and 2.6 ± 0.7 mg L^{-1}. After 30 days of remineralization, the mass loss (after calcinations) for the samples infiltrated with nanoglass was 25 ± 3% (32 ± 3% for microglass) suggesting a higher mineral content. The Young's modulus of the infiltrated samples was not different than demineralized dentine (6.6 ± 1.2 GPa).	Vollenweider *et al*. (2007)[213]
Rod-shaped HA NPs were synthesized by a hydrothermal technique. NPs were 100 nm long and 30—60 nm in diameter.	As a dentifrice for the treatment of dentine sensitivity.	Dentine sections were obtained from human molars and 1 mm thick dentine discs were prepared. Specimens were etched with 37 vol % phosphoric acid solution for 60 s and then infiltrated with 0.5 wt % nano-HA suspensions in methanol. Prior to application suspensions were ultrasonicated for 5 min.	50% of the dentinal tubules were fully occluded and another 40% had at least half of their cross-sectional area blocked by HA NPs.	Earl *et al*. (2006)[98]
Nano-HA. Partide size was not specified.	As a paste to remineralize enamel.	Subsurface enamel lesions were induced to permanent teeth. Specimens were then treated with two toothpastes slurries. Both were prepared by mixing 100 g of toothpaste in 100 mL of distilled water. One slurry contained nano-HA with sodium monofluorophosphate (0.65%) and the other nano-HA but exduded fluoride. Enamel specimens remained static in stirred solutions and tested after 24 or 48 h of remineralization.	The Vickers hardness number (VHN) for sound enamel was 326 ± 25.5 and for demineralized specimens 293.2 ± 18.1. After 24 and 48 h of remineralization with the slurry containing nano-HA and fluoride, the VHN were 298.8 ± 19.7 and 316.7 ± 14.1, respectively. For specimens treated with nano-HA but no fluoride, the corresponding values were 312.3 ± 14.2 and 315.4 ± 14.1.	Jeong *et al*. (2006)[208]

[a] Studies are presented in chronological order for convenience.

TABLE 5. Literature Data on the Toxicity of Engineered Nanomaterials from *in vivo* Oral Exposure Studies[a]

engineered nanomaterial	dose	exposure method	species	toxic effects	author
Au NPs (20 nm) and Ag NPs (20 nm).	1 or 2 M kg^{-1} of each ENM daily.	Exposed once daily for 14 days by oral gavage.	Male Swiss albino mice (25—30 g).	Exposure to the NPs caused body weight loss, which was higher for Ag NPs compared to Au NPs and more evident at the highest concentration (2 M) tested. The blood and tissue (brain, liver, kidney, and spleen) oxidative stress levels were elevated for all groups compared to control showing that both ENMs produced toxicity. Ag NPs were found to be more toxic for all organs except the spleen where Au NPs caused more toxicity. The toxic effect was dose dependent for both NPs.	Shrivastava *et al.* (2014)[265]
^{125}I labeled graphene oxide and polyethylene glycol (PEG) functionalized graphene oxide derivatives.	100 mL of 20 μCi per mouse of ^{125}I, a single dose of 4 mg kg^{-1} of each ENM. Sampling at 1, 7, and 30 days postdosing.	Orally injected with the dispersion, single dose.	Female balb/c mice.	^{125}I labeled PEGylated graphene oxide derivatives show no obvious uptake to the internal tissues oral administration. Radioactivity in the stomach and intestine increased by day 4 postexposure. No changes in hematology were observed.	Yang *et al.* (2013)[266]
<20 nm noncoated (NM300 K), or <15 nm PVP-coated Ag NPs, $AgNO_3$, or carrier solution only (NM300 KDis).	Ag NPs: 90 mg Ag kg^{-1} body weight (bw). $AgNO_3$: 9 mg Ag kg^{-1} bw.	Exposed daily for 28 days by oral gavage. Dosing volume was 3.3 mL kg^{-1} bw.	Male Sprague—Dawley rats, 6 weeks old.	Silver was present in all examined organs with the highest levels in the liver and spleen for all silver treatments. Silver concentrations in the organs were highly correlated to the amount of total Ag in the Ag-NP suspension, indicating that dissolved silver, and to a much lesser extent, Ag NPs, passed the intestines in the Ag-NP-exposed rats. In all groups silver was cleared from most organs after 8 weeks postdosing, but not from the brain and testis.	van der Zande *et al.* (2012)[19]
Poly(amido amine) dendrimers and silica NPs of different size (50—200 nm), surface charge, and surface functionality.	0.2 mL of single escalating doses per mouse were administered starting from 3 or 10 mg kg^{-1} at half-log dose increments (up to 1000 mg kg^{-1}).	All test compounds were dispersed in sterile physiological saline (filtered through 0.2 mm filters) and injected intravenously by tail vein injections. Animals were monitored for 10 days.	CD-1 (caesarean derived-1) mice.	A distinct trend in nanotoxicity based on surface charge and functional group was observed with dendrimers regardless of their size. Amine-terminated dendrimers were fatal at doses >10 mg kg^{-1} causing hematological complications, whereas carboxyl- and hydroxyl-terminated dendrimers of similar sizes were tolerated at 50-fold higher doses. Larger silica NPs were less tolerated than smaller silica NPs irrespective of their surface functionality.	Greish *et al.* (2012)[267]

Table 5. Continued

Al_2O_3 NPs (30 and 40 nm). Al_2O_3 (bulk, size not specified).	ENMs were suspended in 1% Tween-80. Doses of 500, 1000, and 2000 mg kg^{-1}.	Single oral doses (precise method not specified). Animals observed for 14 days.	Adult female albino Wistar rats, 8—10 weeks old.	Aluminum concentrations are not reported in the tissues. Inhibition of hepatic superoxide dismutase at day 3 postexposure, mostly lost by day 14 postexposure. Hepatic catalase increased with no clear difference between the materials. The authors report a dilated central vein and expanded portal tract, but there are no quantitative histological measurements to support the claim.	Prabhakar *et al.* (2012)[268]
Single-walled carbon nanotubes (SWCNT), 1.1 nm mean outside diameter, 5—30 μm length, compared to C60.	Control, 10, or 500 mg kg^{-1} SWCNT or C60 for 6 weeks.	ENMs incorporated into animal feed.	Rainbow trout (*Oncorhynchus mykiss*)	Normal growth and hematology indicated no overt toxicity. A transient oxidative stress was observed in the brain as measured by thiobarbituric acid reactive substances (TBARS). Two animals from the C60 treatment showed liver pathology including necrosis and vacuole formation in the parenchyma.	Fraser *et al.* (2011)[234]
TiO_2 NPs (5 nm).	Control, 5, 10, or 50 mg kg^{-1} every day for 60 days.	Intragastric administration of repeated daily dose.	Mice	The Y-maze test showed that TiO_2 NPs exposure could significantly impair the behaviors of spatial recognition memory. Moreover, TiO_2 NPs significantly inhibited the activities of Na^+/K^+-ATPase, Ca^{2+}-ATPase, Ca^{2+}/Mg^{2+}-ATPase, acetylcholine esterase, and nitric oxide synthase. Cholinergic neurotransmitters were also affected.	Hu *et al.* (2010)[42]
TiO_2 NPs (50 and 120 nm). Crystal structures not specified.	Suspensions of TiO_2 (5 g kg^{-1} bw), lead acetate (500 mg kg^{-1} bw), or combined dosing of the above (TiO_2 + lead acetate) for 7 days.	Oral gavage. 0.1 mL 10 g^{-1} bw, daily for 7 days.	Laboratory-bred Kun Ming mice, female and male, 6—8 weeks old.	Note, food and water provided 2 h after each gavage. Elevation of total Ti metal concentrations in the liver, kidney, and brain at 7 days postexposure. Combined exposure with lead acetate increased the apparent Ti accumulation. Tissue Pb concentrations also increased in the combined exposure. Authors interpret histopathology as "deranged and swollen" cells in the liver, swollen renal tubules, and necrotic cells in the hippocampus. However, the histology was not quantitative with no incidence or criteria for histological reporting described.	Zhang *et al.* (2010)[269]
P25 TiO_2 NPs (21 nm); 75% anatase and 25% rutile.	Control, 10, or 100 mg kg^{-1} TiO_2 NPs diets for 8 weeks followed by a 2 week recovery.	ENMs incorporated into animal feed.	Rainbow trout (*Oncorhynchus mykiss*)	Ti accumulation in gill, gut, liver, spleen, and brain. Adverse effects included 50% inhibition of the brain Na^+/K^+-ATPase activity, but there were no effects on growth.	Ramsden *et al.* (2009)[233]
"Aeroxide" P25 TiO_2 NPs (21 nm); 75% anatase and 25% rutile.	0, 60, 120, 300, and 600 mg L^{-1} concentrations for 5 days.	Drinking water, 5 mL of water intake for average 30 g mouse.	C57Bl/6J*pun*/*pun* adult male mice.	DNA strand breaks indicated by increased tails on alkaline comet assay in peripheral blood cells. Increased micronuclei incidence to about 9/1000 red blood cells. mRNA for pro-inflammatory cytokines up regulated.	Trouiller *et al.* (2009)[270]

Table 5. Continued

TiO_2 NPs (25 and 80 nm), compared to 155 nm material.	5 g kg^{-1} for 2 weeks.	Single oral gavage.	Adult mice	The accumulation of Ti metal from nanoscale TiO_2 (25 and 80 nm) occurred in the spleen, kidney, lung, brain, and liver; depending on particle size. Organ pathologies in the liver were interpreted as hydropic degeneration around the central vein and the spotty necrosis of hepatocytes. Blood urea nitrogen elevated in the 25 nm TiO_2 treatment, interpreted as renal dysfunction.	Wang *et al.* (2007)[231]
Cu NPs (23.5 nm), Cu microparticles (17 μm), or $CuCl_2$ metal salt.	Control, 500−5000 (micron powder), 108−1080 (nano), 24−237 (metal salt), in mg kg^{-1}.	Single oral gavage.	Imprinting control region (ICR) mouse model, 8 weeks old.	The LD_{50} values for the nano and , microcopper particles, and $CuCl_2$ were 413, >5000, and 110 mg kg^{-1} body weight, respectively. Nanoscale material caused atrophy of the spleen with fibrosis. Mild steatosis reported in the liver, and moderate tubular necrosis in the kidneys of Cu NP-exposed mice.	Chen *et al.* (2006)[232]

[a] Studies are presented in chronological order for convenience.

derived from the effects of charge screening by electrolytes on the protein folding of mucins.[37] Provided the ion concentrations remain at millimolar levels, the effects of ENMs on the rheology of saliva are expected to be small. For similar reasons, the general pH buffering in saliva from millimolar concentrations of phosphate and bicarbonate might also be unaffected. However, ENMs often have a high surface area to volume ratio, and it is possible that solutes such as fluoride, that are only present at micromolar concentrations, could be adsorbed by some ENMs. The F^- ions in saliva can react strongly with the free Ca^{2+} and HPO_4^{2-} ions available in the hydroxyapatite (HA) of enamel to form fluorapatite crystals that are less soluble and more resistant to acids compared to pure HA (Figure 1B). This is one of the benefits of fluoride in preventing dental caries, and theoretically this function may be lost, especially with ENMs with a net cationic charge in the saliva. Unfortunately, the effects of ENMs on the bioavailability of important trace anions have not been investigated.

The salivary flow rate also controls the solute concentrations in the oral cavity. Factors such as age, diseases, and medication can impair the quantity (and quality) of saliva. The reduction or absence of the salivary flow usually results in increased food retention, and when the salivary buffering capacity has been lost, an acid environment is encouraged causing enamel demineralization. In a healthy person, the unstimulated (resting) salivary flow rate is 0.3−0.4 mL min^{-1} and may increase to 1.5−2.0 mL min^{-1}.[34] When saliva is initially secreted, it is sterile, but subsequently the bacterial concentration can reach 10^9 mL^{-1}. Salivary flow rate is normally too high to allow bacterial growth and proliferation in the fluid.[38] Instead, bacteria need to adhere on an oral surface (teeth, mucosal tissue) to survive in the long term. The secretion of saliva is mainly controlled by cholinergic parasympathetic innervation to the salivary glands, which promotes the release of saliva from the acinar cells, while in contrast stimulation of sympathetic nerves tends to increase the protein content, resulting in a more viscous saliva.[39] Evidence suggests that direct application of high milligram concentrations of ENMs to isolated nerve preparations does not alter the ability of peripheral nerves to generate an action potential,[40] but the effects of ENMs on the secretory activity of salivary glands have not been investigated.

Saliva also contains immunological components (*e.g.*, IgA, IgG, and IgM) and antibacterial proteins (*e.g.*, lysozyme, lactoferrin, and peroxidases). The effects of ENMs on the bioavailability and function of these immune-related components of saliva have not been specifically investigated. However, immunoglobulins and complement factors involved in immunity

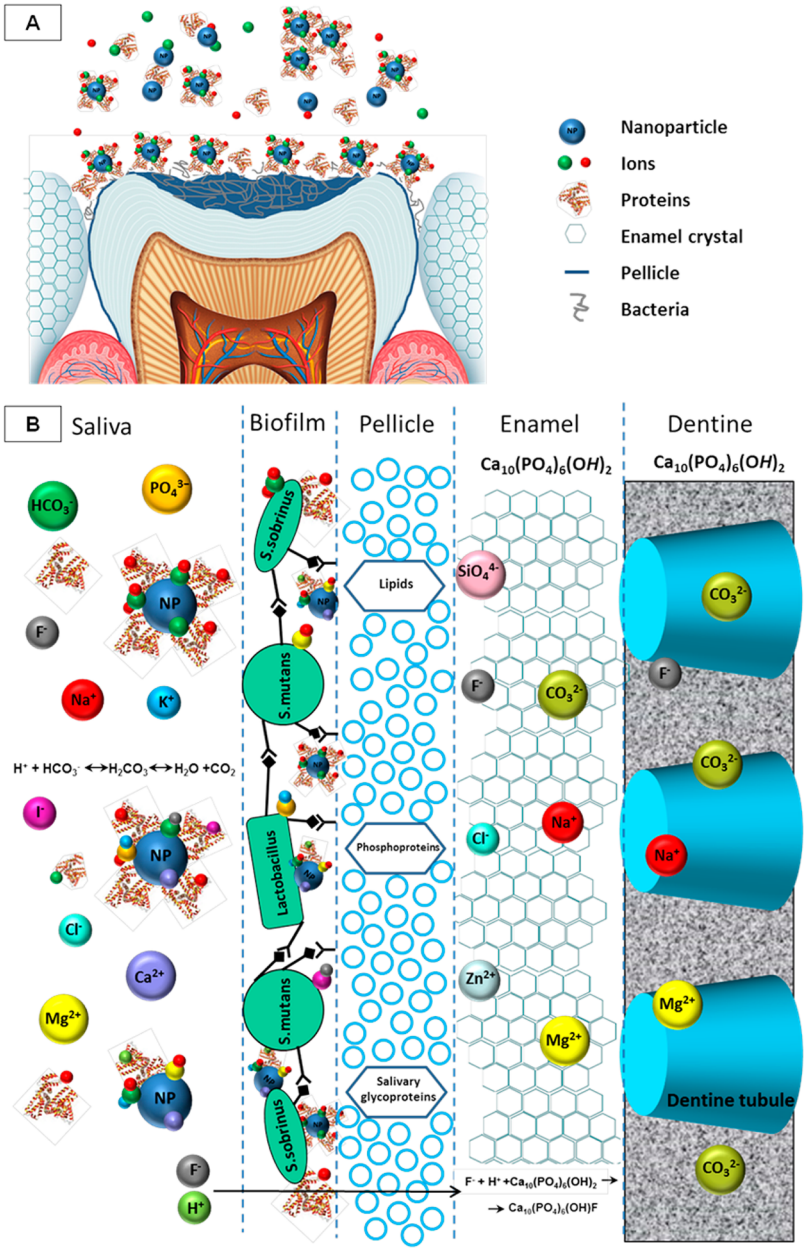

Figure 1. (A) Diagram shows the presence of NPs (isolated particles or agglomerates) in saliva and the structure of dental tissues. The pellicle covers the superficial layer of enamel, and the oral biofilm develops on the pellicle surface. The characteristic hexagonal shape of the enamel crystallites is apparent and also the presence of the dentinal tubules in the underlying tissue of dentine. The NP−ion−protein complexes do not adhere directly to the tooth surfaces, but adhesion occurs either to the pellicle layer or the developing biofilm. (B) Schematic diagram of the oral environment, oral biofilm, and dental mineralized tissues showing the distribution of NPs and ions. Natural saliva normally contains a range of ions and proteins. In the presence of NPs, NP−ion−protein complexes are formed. Oral conditions promote particle agglomeration that results in particle sedimentation onto the dental surfaces. The pellicle has a globular structure and its proteinaceous layer facilitates the adherence of the early colonizing species necessary for the oral biofilm development. The oral biofilm and pellicle act as diffusion/permeation barriers to NPs preventing them from reaching the enamel−pellicle interface. Certain ions (F^-, Cl^-, SiO_4^{4-}, Zn^{2+}) are more abundant near the external surface of enamel, while others (Na^+, Mg^{2+}, CO_3^{2-}) are found at higher concentrations near the dentino−enamel junction. The most commonly ions found in dentine are F^-, Na^+, Mg^{2+}, and CO_3^{2-}.

from serum do adsorb to ENMs, depending especially on the surface charge and hydrophobicity of the material.[41] Lysozyme is also adsorbed onto the surface of some ENMs resulting in an alteration of the spatial arrangements of the β-sheets in the enzymes tertiary structure with a likely loss of its antibacterial properties (*e.g.*, TiO_2[42]). In contrast, some ENMs have peroxidase-like chemical reactivity,[43] and such materials could be exploited for their antimicrobial properties. There are numerous other organic components in saliva including the mucin glycoproteins, agglutinins, histatins, proline-rich proteins, statherins, and cystatins.[44] The effects of ENMs on many of these proteins/peptides are unknown.

TOOTH SURFACE MICROENVIRONMENT AND INTERACTIONS WITH ENMS

Substances in saliva do not interact directly with the tooth enamel, but do so via a thin layer known as the pellicle, which usually covers the dentition (Figure 1A,B). The pellicle is an acellular proteinaceous film of salivary origin that is usually formed within minutes, and it is so strongly adhered to the enamel that even tooth brushing does not remove it. The thickness of the pellicle is 10−20 nm within a few minutes, increases to 20−500 nm at 2 h, and reaches 100−1300 nm at 24 h.[45] The main constituents of pellicle are salivary glycoproteins, phosphoproteins, lipids, and to a lesser extent, components from the gingival crevicular fluid.[46,47] The pellicle plays an important role in the tooth demineralization and remineralization processes because it passively controls the diffusion of ions in and out of the dental tissues. It is therefore a selective semipermeable structure that is regarded as a chemical buffering barrier, protecting the mineral content of the enamel from bacterial[48] and dietary acid demineralization.[49,50] However, the structure of newly formed pellicle may not prevent the penetration of ENMs. The enamel−pellicle interface is not a homogeneous film, but has a multilayered globular structure.[51] The size of these spherical structures ranges between 25 and 125 nm in diameter, and quite often voids are also observed, as the distance between adjacent globules is from 8 to 85 nm (sizes and distances measured from electron microscopy images of a 2 h pellicle[52]). It is therefore theoretically possible that ENMs smaller in size than these voids could penetrate the pellicle as it forms. However, once the proteinaceous biofilm is present over the globular structure of the pellicle, it seems likely that steric hindrance and protein−ENM interactions would slow or prevent further diffusion of the ENMs into the pellicle layer.

The formation process of the proteinaceous pellicle layer is not fully understood, but is presumably governed by the colloidal and physicochemical properties of the macromolecules in saliva, such as the charge density, hydrophobicity, and relative concentration of each component to compete for binding on the tooth surface. Much the same ideas apply to the formation of the "protein corona" on ENMs in complex body fluids such as serum.[53−55] It is therefore logical that any ENMs present in the saliva will compete with the pellicle surface for proteins and other macromolecules in the saliva. The newly formed protein corona of ENMs (Figure 1A,B) will inevitably alter their physicochemical properties. For example, adsorbed proteins may alter the net surface charge on the ENMs (changes in zeta potential and isoelectric points of NPs[56]); and consequently the charge screening with electrolytes and the agglomeration behavior of the ENMs in the saliva itself. In theory, the interactions of the coated ENMs with the pellicle will also be influenced. It also follows that a tooth coated with an ENM of defined surface chemistry could be used to manipulate the formation of the pellicle. The latter may be of interest for preventing microbial colonization of the teeth, for example, by providing a surface that does not favor microbial adherence. Bacteria are probably nonspecifically associated with the tooth surface (Figure 1B) under the effect of van der Waal's attractive forces as well as attractive or repulsive electrostatic, hydrogen bonding, and Brownian motion forces.[29] Surface hydrophobicity generally enhances the attachment of microbes, and consequently a hydrophilic ENM coating might reduce the attachment of microbes.

Numerous studies have examined the antibacterial effect of NPs incorporated in the matrix of dental materials against mostly individual oral pathogens (see Table 1), while other research groups have investigated the antibacterial activity of NPs suspended in biological media containing microbes.[57,58] However, the antimicrobial effects of ENMs in complex clinically relevant biofilms such as those on the pellicle are far from clear. In general, the microbial communities in natural biofilms tend to be more resilient than the artificial cultures of individual species of microbes in the laboratory. For example, while Ag NPs are known for their antimicrobial properties on *S. mutans*,[36,58] the same material has no effect on the natural microbial diversity in marine biofilms that also include *Streptococcus* species.[59] The biodiversity of gut microflora is also influenced by metallic ENMs in some animals (*e.g.*, fish gut[60]), but a similar understanding for the oral cavity biofilm of humans is lacking.

Although some ENMs may be small enough to theoretically permeate into the porous mineral structure of the enamel−pellicle interface (above), it is likely that the biofilm formed on the pellicle will be a significant barrier to ENM diffusion; either through steric hindrance (*e.g.*, ENMs becoming entrapped or entangled in the biofilm protein matrix) or by adsorption of the ENM onto the glycoprotein coat of the S-layer of microbes.[61] Permeation into biofilms is partly controlled by biofilm thickness. Diffusion works most efficiently over small distances of a few microns and is exponentially slower for small increases in particle diameter.[62] The diffusion path through the biofilm will also be determined by the microarchitecture of the biofilm; which is defined by the participating species and the conditions under which the biofilm is developed (potentially, every biofilm is unique in this respect). Channels and voids are known to be present in the oral biofilm. Plaque models have shown that the open channels can be 300 nm in diameter,[63] which theoretically would be large enough to allow ENMs to permeate. However, diffusion theory based on the original Fick equations is idealized and does not take into account solvent drag or steric hindrance from proteins in the biofilm. Consequently, even small NPs

(<20 nm) may find it difficult to penetrate the biofilm. For example, Thurnheer *et al.* found that 240 kDa molecules had difficulty in infiltrating the oral biofilm.[64] The volume occupied by a molecule of this size is approximately 290 nm^3, and thus, it would be equivalent to a spherical NP of just 4 nm in diameter.

Furthermore, it is also likely that the ENMs diffusing into the biofilm will not be pristine, but coated in macromolecules and electrolytes from the saliva. Although the protein corona formation on ENMs in saliva has not been specifically studied, chemistry would suggest (for example) that the polyanionic mucins in saliva would bind electrostatically to cationic ENMs and/or that the bulk electrolytes in saliva will form an electric double layer on the surface of the particles.[31] The process is also likely to be dynamic with microbes secreting proteinaceous material as the biofilm develops and the bulk fluid moves into the pellicle enabling some adsorption of ENMs into the biofilm (the latter adsorption partly being governed by unstirred layer formation in the case of solutes[65]).

Nonetheless, understanding of how EMNs coated in a salivary corona will interact with the biofilm, and the microbes within it, is a significant data gap in quantifying the bioavailability of oral ENMs. Experiments are needed to determine the details of how the adhesion of ENMs on the dental surfaces is regulated, as well as the likely complex interactions of the ENMs with the bacteria, their secretory products, and the proteins forming the underlying pellicle layer. Currently there are no computational models for ENM binding to biological surfaces, but ENM adhesion or adsorption is likely to be governed by the chemistry of the pellicle and overlying biofilm (plaque) since the ENMs would not be in direct contact with the chemistry of the enamel surface. Any such biotic ligand type-model would need to consider the effects of the ionic strength and its likely ability to erode the electric double layer on the particle surface;[31,66,67] the role of protein corona formation to sometimes encourage colloidal stability[68−70] or alternatively promote agglomeration[71−73] depending on the precise mixture of ions and macromolecules present in the media. ENMs can also impose structural and functional changes to the adsorbed proteins,[74] although the functional consequences for the saliva, pellicle, and biofilm remain to be investigated.

INTERACTION OF ENMS WITH THE FINE STRUCTURE AND CHEMISTRY OF THE TOOTH

The gross anatomy and fine structure of human teeth are well-known,[75] but here the anatomical and chemical characteristics of the tooth are considered in the context of potential interactions with ENMs (Figure 1). Teeth consist of four different tissues of which three are mineralized (enamel, dentine, cementum) and surround an inner core of loose connective tissue; the fourth tissue, known as the dental pulp (Figure 2). The chemical composition of each tissue is outlined below.

Enamel. Enamel covers the crown of the tooth and is the hardest and most densely calcified tissue in the body. Its thickness varies as a function of location and age in the tooth[76] and can be between 2.6 mm over the cusps of sound mature teeth and as low as 1.2 mm on the lateral surfaces.[77] Ninety-six percent of the enamel by weight consists of mineral, with water and organic material composing the rest.[78] Calcium hydroxyapatite ($Ca_{10}(PO_4)_6(OH)_2$) is the most dominant constituent of enamel, although minor (<2%) nonapatitic mineral phases, such as octacalcium phosphate, can be detected. Calcium hydroxyapatite (HA) does not always exist in its pure form, but commonly other variations are also present. Calcium ions (Ca^{2+}) and hydroxyl groups are frequently missing and thus replaced by other ions present in the enamel such as fluoride (F^-), carbonate (CO_3^{2-}), chlorine (Cl^-), silicon (usually as SiO_4^{4-}), sodium (Na^+), magnesium (Mg^{2+}), and zinc (Zn^{2+}). The distribution of these ions is not even across the enamel layer (Figure 1B). Some of them (F^-, Cl^-, Si, Zn^{2+}) appear at higher concentrations near the external surface of enamel, while others (Na^+, Mg^{2+}, CO_3^{2-}) are more abundant near the dentino−enamel junction (DEJ).[79,80] Enamel apatite is highly crystalline, with the crystals being at least 100 μm long, 30 nm wide, and 90 nm thick.[81] Most crystals are hexagonal (Figures1A,B) but some can be distorted due to crowding. Dental enamel has 558 crystallites/mm^2 near the tooth surface[82] and the distance between adjacent crystallites is 20 nm.[83] HA crystals are surrounded by a thin film of firmly bound water (2 wt %). The presence of water is associated with the porosity of the tissue. The remaining 2 wt % in mature enamel is the organic matrix. Enamel does not contain collagen, but it has two unique classes of proteins called amelogenins and enamelins.

The ability of ENMs to permeate or adhere to the tooth enamel is poorly understood. Enamel is permeable to electrolytes, although in this dense and highly mineralized tissue this is most likely via intercrystalline spaces, rod sheaths, and other defects in the surface.[84−86] Nguyen *et al.* confirmed some innate permeability of human enamel using the Brunauer−Emmett−Teller (BET) gas adsorption method giving a BET surface area, pore volume, and pore size of 0.22 $m^2\ g^{-1}$, 2.8 $mm^3\ g^{-1}$, and 22 nm, respectively.[87] There appears to be no data showing whether or not ENMs are capable of permeating enamel. However, Li *et al.* report the use of 20 nm HA particles to repair dentinal enamel.[88] Cai *et al.* also suggested that HA NPs with sizes <20 nm could integrate with the surface of enamel matrix, but highlighted the importance of particle size with the use of 20 nm particles being more advantageous than 40 or 80 nm HA particles.[89] The exact type of bonds developed between ENMs and the enamel

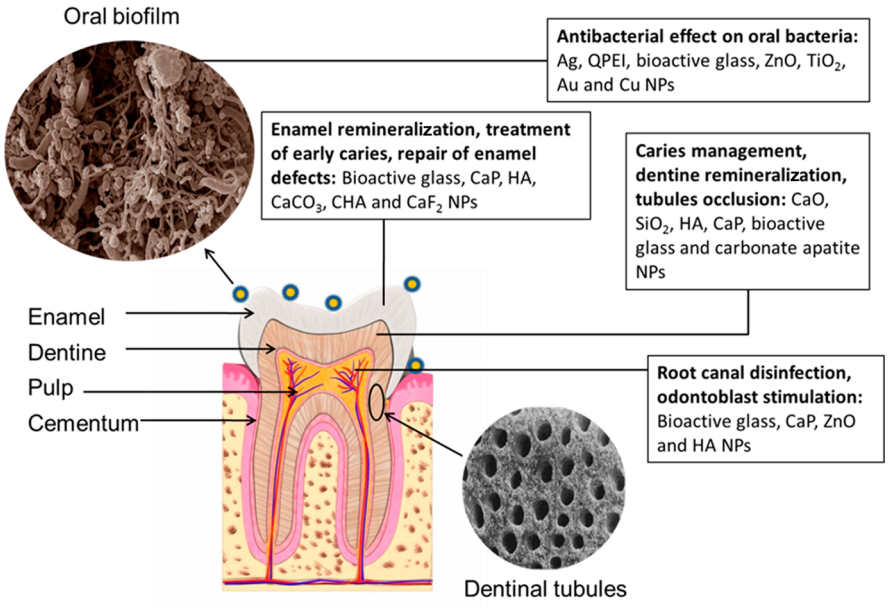

Figure 2. Tooth anatomy showing the four main components of the tooth (enamel, dentine, cementum, and pulp). Details of the complex oral biofilm, which develops on the tooth surfaces, and the characteristic microscopic channels (dentinal tubules) that permeate dentine are also shown. Dental research studies have investigated the use of a big range of ENMs in different clinical applications including enamel remineralization strategies, antibacterial applications, caries management, dentine hypersensitivity, and root canal disinfection.

remains unclear, although it seems probable that electrostatic and van der Waals forces will be involved.[90,91]

Dentine. Dentine is about 70% inorganic, 20% organic, and 10% water by weight.[92] The mineral phase is HA, similar to enamel, but dentine crystals have a lower calcium content and are more carbonate-rich compared to stoichiometric HA. The crystallites are much smaller than those found in enamel, having a hexagonal or plate-like morphology, and with dimensions of 3−30 nm in cross-section and about 50 nm in length.[93,94] The HA crystals are therefore naturally occurring nanostructures, and with high concentration of carbonate (4.6 wt %) renders the dentine a large and chemically reactive surface area.[95] Fluoride, sodium, and magnesium have also been detected in dentine in small amounts (Figure 1B). The organic part of dentine is mainly type I collagen that provides the structural backbone, which holds together the apatite crystallites. The fibril diameter in dentine collagen varies from 60 to 200 nm.[96]

Dentine is permeated by characteristic microscopic channels called dentinal tubules (Figures 1B and 2). Their diameter ranges from 2.5 μm near the pulp, to 1.2 μm in the middle of dentine, and 900 nm near the DEJ.[97] The tubule density also varies depending on location. The number of tubules near the pulp is 45,000 mm^{-2} covering 22% of the total surface area of dentine, in the mid portion there are 29,500 mm^{-2} tubules, and the corresponding value near the DEJ is 20,000 mm^{-2} where the percentage of the dentine surface area occupied by dentinal tubules is just 1%.[95,97]

The application of ENMs to dentine has received more attention (see Dentifrices and Personal Care Products section) compared to enamel (Table 4); mainly because dentine remineralization is not so predictably achieved. Dentine is more porous than enamel due to its organic components, higher water concentration, and the presence of dentinal tubules. Consequently, ENMs of larger diameters are more likely to infiltrate dentine than enamel. Earl *et al.* managed to infiltrate dentine tubules with 100 nm HA particles finding that the shape of the ENMs was also important.[98] In the same study, larger needle-like HA particles up to 600 nm in length and 30−60 nm in width showed very limited infiltration. When demineralized dentine was treated with HA nanorods having an average size less than 100 nm (variation in particle length was between 30 and 145 nm), 50% of the tubules at the dentine surface were fully occluded and an additional 40% were partially occluded.[99]

Most studies investigating the infiltration of dentine with ENMs use a partially demineralized dentine model. Consequently, interfibrillar and intrafibrillar infiltration is also possible as removal of the inorganic components during demineralization results in larger voids between the collagen fibers.[100] Using a fully demineralized model instead, Besinis *et al.* achieved an extensive infiltration of the dentine collagen network with spherical HA and silica NPs when the particle size was less than 15 nm in diameter;[101] in agreement with measurements of the interfibrillar spaces after demineralization between 20−25 nm.[102,103] In a follow-up

study, Besinis *et al.* confirmed the remineralization potential of fully demineralized dentine following infiltration with HA and silica NPs.[104]

Cementum. Cementum is a thin specialized calcified, fibrillated bone substance that covers the dentine of the root (Figure 2). By weight, the cementum is approximately 65% inorganic material (mainly HA), 23% organic (collagen type I, proteins, and polysaccharides), and 12% water. The HA crystals in cementum are thin and plate-like with an average size of 55 × 8 nm. The thickness of cementum is considerably higher at the root apex (50−200 μm) compared to the cervical part of the tooth (10−15 μm).[105] There appears to be limited studies of ENMs on the cementum layer of the tooth or on the cementocytes (*e.g.*, effect of bioactive glass NPs on cementoblasts[106]).

Pulp. Pulp is located in the pulp chamber, which occupies the central portion of the tooth (Figure 2). The nerves present in the pulp allow detection of external stimuli and account for the sensation of teeth. The main function of the pulp is the formation of dentine.[107] The odontoblasts that are responsible for the formation of dentine lie along the periphery of the pulp tissue. Other cells present in the pulp include fibroblasts, preodontoblasts, macrophages, and T lymphocytes.

One prospective area of research for the dental pulp is the use of ENMs in regenerative medicine. Pulp stem cells can be used as a restorative clinical treatment to regenerate both the pulp and vasculature in the tooth.[108] Dysfunction of stem cell differentiation is also generally implicated in DNA damage and tumorgenesis in the head and neck.[109,110] ENMs have been proposed for medical imaging of stem cells (iron NPs, quantum dots) in order to track the migration and differentiation of the cells, as well as the use of nanofiber scaffolds to aid the regeneration of pulp tissue.[17] Naturally occurring nanostructures such as nanotoliths with bacterial cellulose have also been proposed as scaffolds for pulp regeneration.[111]

CURRENT STRATEGIES FOR CLINICAL DENTISTRY: A ROLE FOR ENMS?

The etiology of pathogenesis in the oral cavity is complex, and a primary strategy for dentistry is the prevention of disease. Oral hygiene instructions for the patient is the first attempt in preventing both carious lesions and periodontal disease.[112,113] Clearly, the use of antibacterial and/or abrasive ENMs in toothpaste may aid teeth cleaning. However, ultimately, the dental pellicle is the natural barrier that protects the hard tooth structures and the supporting tissues from the adverse effects of microorganisms and their corrosive metabolites.[114] The antibacterial properties of some ENMs could be used to supplement the natural immune defenses (*e.g.*, immunoglobulins, lysozyme) already present in the pellicle. The dental pellicle, however, is also the structure in which bacterial colonization begins. Perhaps ENMs can be designed to act as receptors for species-specific bacterial adhesion to the tooth surface; in essence, using ENMs as a "probiotic" surface to promote healthy microbes in the pellicle, or to aid in the restoration of a normal biofilm following dental treatment. The demineralization of the tooth structure caused by acidic bacterial metabolites might be ameliorated by the use of alkali ENMs, which, for example, might slowly release phosphate or bicarbonate buffering by dissolution (pH control at the tooth surface). The inflammation of the soft tissue by factors such as lipopolysaccharides (LPS) released by bacterial infection in the biofilm[115] may be hard to prevent with specific chemical buffering because of the diversity of bacterial exudates. Nonetheless, metallic ENMs do absorb LPS very well[116] and might reduce the bioavailability of this inflammatory agent.

Furthermore, dietary abrasion of enamel during mastication has been hypothesized to release naturally occurring nanoscaled HA particles, which are known to reduce oral biofilm formation and produce a remineralization effect to prevent carious lesion progression.[117] With soft diets of today consisting of less protein and increased carbohydrates, the release of protective nanoscale HA is likely to be in decline; contributing to growing incidence of caries in the human population.[117−120] Potentially, toothpastes and other oral hygiene products could be supplemented with engineered nano-HA to combat this problem, but the underlying cause of poor diet also needs to be addressed.

The dental materials of today are greatly challenged by secondary disease (*e.g.*, recurrent caries) after initial treatment, one of the main reasons for failures in dental materials.[121−124] For this reason, an interest in the bioactivity of dental materials is increasing, as materials need to go beyond the physical and mechanical aspects of tissue repair. In direct tooth restoration with new composite materials, mechanical properties such as wear resistance, surface hardness, fracture toughness, and compression, tensile and flexural strengths are required to meet demands in the oral environment and be sufficient to withstand masticatory forces.[125−127] While improvements in these areas are being accomplished for direct restorative materials, several limitations still exist in modern materials.[127] The difficulties include adapting the material to the internal surfaces of a prepared cavity, creating an effective marginal seal at the cavity−tooth interface, marginal deterioration over the life of the restoration, material discoloration over time, secondary decay caused by material microleakage, and postoperative sensitivity.[128,129] Nanotechnology has the potential to bring improvements in the physical and mechanical properties of dental materials, but the bioactivity aspect should not be overlooked. This might include biocidal

properties of ENMs and ENMs coated in factors to promote a beneficial immune response in the diseased tissue (*e.g.*, cytokines, compliment activation), and subsequently growth factors to promote angiogenesis and wound repair.

Restorative dentistry has traditionally focused on the use of dental materials to replace tissue in the oral environment in order to restore physical function following tissue loss from disease processes.[130] Although success with respect to mechanical function is often achieved, the broader biological function of the tissue is not. The mechanical and biological properties of living teeth are intimately related. Odontoblasts are key cells in tissue regeneration and function in tertiary dentine development to protect the vital pulp from any continuation of disease processes or trauma.[131,132] New ENMs that promote pulpal cell repair and cell differentiation may increase dental pulp vitality during or after restorative processes and ultimately improve oral health.

In the periodontium, regeneration of bone that has been lost due to periodontal disease could be a vital step in the cessation of disease itself; where periodontal pocketing creates disease-promoting architecture in the oral environment.[133] For example, engineered nanostructures could be used as a bone replacement,[134] or ENMs that promote osseointegration (*e.g.*, coated with HA) and/or bone regeneration could be used. In the 1990s it became apparent that enamel matrix proteins (EMPs) could promote fibroblast proliferation and growth, and commercial products, such as the enamel matrix derivative Emdogain, and similar products that contain factors, such as amelogenin, are used in new regeneration therapies for tissue loss caused by periodontal disease. The use of such derivatives highlights the importance of bioactive materials in modern therapeutic strategies against periodontitis.[135] The use of ENMs to provide a more targeted drug delivery of such therapeutics in dentistry has yet to be explored.

ENGINEERED NANOMATERIALS AND THEIR USE IN DENTISTRY

Antibacterials and Infection Control. Silver, zinc, and copper have been traditionally used as antimicrobial agents for many centuries. Metals and their oxides have been incorporated in a wide range of dental material applications, either alone or in combination with other components;[136] and there is interest in replacing the traditional micron-sized antimicrobial metal powders with their nanoscale counterparts (Table 1). The superior bactericidal activity of ENMs is attributed to their increased surface area and the possibility to interact directly with the bacterial cell wall because of their small size. Nanoparticulate silver is the most favorable antimicrobial agent among the metals;[137−140] followed by TiO_2.[124,141] Zn and ZnO NPs have also been suggested for use in dental applications due to their antibacterial properties.[142,143] However, the number of the applications of nanometals in dentistry is limited, and for example, Zn does not have the acceptance it has in other fields such as the food industry.[144] CuO is cheaper than Ag, with the advantage of being a stable chemical and with physical properties that allow it to be easily mixed with polymers.[145] However, Cu NPs have not been fully investigated as potential antibacterial agents in dental materials. Similar arguments apply to Au NPs.

Ag NPs may be favored over other nanoparticulate metals because silver is more bactericidal, while equally hard. In a comparative study, Besinis *et al.* showed that Ag NPs are more antibacterial against cariogenic bacterial species when compared to other metal NPs.[58] Ren *et al.* found the minimum bactericidal concentration (MBC) of Ag, ZnO, and CuO against *Pseudomonas aeruginosa* to be 100, >5000, and 5000 μg mL^{-1}, respectively.[145] The corresponding MBC values against *Staphylococcus aureus* were 100, 2500, and 2500 μg mL^{-1}; confirming the supremacy of Ag NPs. At the same time, silver, copper, and zinc all score 2.5−3.9 on the Moh's scale of hardness (titanium scores 6.0).

The size and shape of metal ENMs may also affect their bactericidal activity. Materials with a particle size of less than 10 nm have been shown to be the most effective against bacteria,[146,147] while triangular NPs may be more bactericidal compared to those with spherical or needle-like morphology.[148] Conversely, Suwanboon *et al.* found the antibacterial activity of ZnO NPs of different shapes (nanorods, platelet-like, nanoflowers) to be similar.[149] Metal-containing NPs are not the only type of ENMs known to provide antimicrobial properties to dental materials. Quaternary ammonium polyethylenimine, chitosan, silica, and bioactive glass NPs have also been suggested.[150−152]

The choice of antibacterial ENMs mainly depends on the type of dental application. For example, Ag, Zn, and TiO_2 NPs are commonly incorporated in resin-based composites or used as antimicrobial coatings for dental materials and implants; while others such as bioactive glass nanopowders are mostly used as root canal disinfectants (Table 1). Silica NPs have been reported to inhibit bacterial adherence and control the growth of the oral biofilm.[153,154] Although silica NPs have no inherent bacterial toxicity, it is likely that it is the unfavorable substrate (surface morphology and chemistry of silica NPs) that prevents or delays bacterial adherence and biofilm proliferation. The antimicrobial activity of some ENMs can be enhanced with UV light (*e.g.*, crystalline TiO_2 NPs[124]). Certain metallic NPs (*e.g.*, Ag and Cu NPs) have been proved effective against a wide range of bacterial strains including *S. mutans*, *S. aureus*, *P. aeruginosa*, *E. coli*, *E. faecalis*, *S. sobrinus*, and *S. epidermidis*,[155,156] while others are more

bacteria-specific depending on their mechanism of action (*e.g.*, ZnMgO NPs show highly specific antibacterial activity to Gram-positive bacteria[157]).

In order for ENMs to be generally accepted as replacements for the traditional antibacterial agents, they must first satisfy the regulatory requirements of any potentially new therapeutic of being safe, or safer than the existing product, and more effective.[158] Additionally, any therapeutic agent should not compromise the integrity of the dental materials. Confidence in new nanotechnology may come from using ENMs as carriers for traditional antibacterial agents; for example, composites based on the release of chlorhexidine, the active ingredient in mouthwashes.[159] However, such an approach may suffer from the short-lived effectiveness of chlorhexidine.[160] In contrast, impregnation of bactericidal NPs into resin-based composites has demonstrated a long-lasting effect against cariogenic bacteria without affecting the physical and mechanical properties of the dental material.[137]

Nanofillers. Some selected examples of the use of ENMs as fillers in dental composites are shown in Table 2. Dental composites generally consist of three main components that are chemically different from each other: the organic matrix (usually a synthetic monomer or resin), the inorganic matrix (the filler), and a coupling agent (usually silane) to bond the filler to the organic matrix. Each of these phases can be modified, and the resultant combination of the three components determines the physical, chemical, mechanical, and optical properties of composites, as well as their clinical behavior. The introduction of new materials in the past few years, such as phosphine oxide initiators and monomethacrylate diluents,[161] has led to dental composites with improved properties. However, it was not until the introduction of nanofillers where significant new advances in the composites were achieved (Table 2).

The chemistry, the morphology, and the size of filler particles used in dental composites vary significantly, even within the nanoscale (Table 2). However, the aim of incorporating fillers to the resin, regardless of the type of filler, is to optimize the properties and performance of the final restorative material. The addition of fillers can enhance the mechanical properties of composites, reduce the polymerization shrinkage, modify the thermal expansion coefficient of the composite to match that of the tooth, improve handling, provide radio-opacity, and provide the composites with wear resistance and translucency.[162] Conventional composites contain a range of fillers including silica, quartz, and radiopaque silicate particles based on the oxides of barium, strontium, zinc, aluminum, and zirconium.[163] A widely accepted classification based on filler particle size was proposed by Lutz and Phillips, where composites are distinguished as macrofiller composites (0.1−100 μm), microfiller composites (0.04−0.1 μm), and hybrid composites (fillers of different sizes).[164] However, resin-based composites can be classified either according to their composition or the filler particle size.[165]

Most of the current conventional composites have a filler particle size in the range of 0.04−0.7 μm. The concern is that particles of these sizes cannot interact optimally with the nanoscopic (1−10 nm) structural elements of enamel and dentine, such as the enamel rods, HA crystals, dentinal tubules, and collagen fibers.[166] As a result, the adhesion between the restorative material and the tissue can be compromised. However, the manufacturing of new advanced composites with unique properties became possible with the introduction of nanofillers (particle size 1−100 nm, Table 2). The smaller particle size diminishes polymerization shrinkage, offers more uniform particle distribution, allows a higher filler load, reduces viscosity, and offers better handling, while the mechanical properties remain sufficiently competent.[166] The average filler size in nanocomposites is 40 nm, but this is not a breakthrough as the same filler size had been achieved with the so-called "microfilled composites" since the 1970s. The real innovation with nanofillers is their ability to increase the load of the inorganic phase. Microfilled composites have a 50 wt % filler load compared to 80 wt % for the nanofilled.[167] Filtek Supreme (3 M ESPE, St. Paul, MN, USA) was the first dental nanocomposite to be launched in the market in 2002. Other examples of commercially available nanocomposites are Premise (Kerr/Sybron, Orange, CA, USA), GrandiO (Voco, Cuxhaven, Germany), Ceram-X (Dentsply DeTrey, Konstanz, Germany), 4 Seasons (Ivoclar Vivadent, Schaan, Liechtenstein), and Palfique (Tokuyama Dental Corp., Tokyo, Japan).

Adding nanofillers to enhance the physical and mechanical properties of resin-based composites is advantageous, and incorporating the highest possible percentage of filler content is the ultimate aim. However, the maximum filler load should be carefully considered because there are limitations. Table 2 shows that the effect of nanofillers on the mechanical properties of composites has received special attention. Some of the mechanical properties commonly measured include microtensile bond strength, flexular strength, diametral tensile strength, fracture toughness, microshear bond strength, Vickers hardness, and compressive strength.

Lohbauer *et al*. found that elevating the concentration of zirconia nanofillers in either the primer or the adhesive gradually increased the microtensile bond strength.[168] Although the highest values were reported for 20 wt % filler content, even specimens with a low filler profile (5 wt %) had enhanced mechanical properties compared to the unfilled controls. Other research groups have also reported that composites had better mechanical properties when they contained nanofillers at a higher concentration.[169−172]

However, there does appear to be an optimal maximum of the percentage of nanofiller in the resin composites, after which the mechanical properties do not improve further, or even deteriorate. In some cases, the mechanical performance declined to such an extent that the unfilled controls were superior.[169,171,173] The optimal filler load varies significantly between materials and was about 10 wt % for CaF_2, 0.2 wt % for HA, 0.5 wt % for sodium montmorillonite (Na-MMT), and 40 wt % for silica nanofillers (Table 2).[169−172] However, some caution should be used when comparing the optimal filler load across ENMs because the studies so far have not used standardized methodologies to prepare the composites; each necessarily requiring a different NPs synthesis, types of resin, modifications of the particle surface, and the timing of the polymerization process. Nanofilled composites may not always enhance mechanical properties compared to microfilled composites. Ruttermann *et al*. found that solubility and shrinkage were similar for both types of composites, but the nanofilled composites demonstrated higher water sorption and opacity.[174]

Although spherical nanofillers are popular, partly because they distribute stress more uniformly across the bulk volume of the composite resin and inhibit crack formation;[166] CNTs have also been investigated. Zhang *et al*. synthesized a composite based on single-walled carbon nanotubes (SWCNTs).[175] The result was a nanocomposite with improved mechanical performance. SWCNTs are well-known to have exceptional strength, but they can also be accepted at higher filler concentrations by resin systems due to their unique dimensional distribution (aspect ratio >1000).[176] Further research should be encouraged on resins accommodating CNTs.

The aesthetics of the composite is also a critical issue for patients, and for example, color matching with the patients natural teeth is desirable. NPs have been employed to modify the translucency for improved aesthetics.[177] However, the optical properties are also of clinical importance, and nanofillers have been used to match the radiopacity of dental adhesives[178] and to reduce the working and setting times for resins.[173] Clearly, nanofillers can improve some material properties while compromising others in the overall nanocomposite. The practitioner should therefore take an overview of the composite in the context of clinical considerations, which are mainly determined by the position of the cavity and the aesthetic requirements.[163]

Dental Implants. The aim of the dental implant manufacturer is to provide a product with a high success rate after the initial implantation and longevity. At present, the failure rates are 5−10%, mainly due to poor osseointegration, infection, or rejection.[179] The future of a dental implant is dictated by the inflammatory response and the behavior of the tissue at the tissue−implant interface in the individual patient. Consequently, the implant surface chemistry and topography are fundamental aspects to be considered when designing an implant. Cells are typically around 10 μm in diameter, but the cell parts are much smaller, in the submicron scale. The proteins secreted during osseointegration are even smaller with a typical size of just 5 nm; which is close to the dimensions of the smallest man-made NPs.[180] The notion of ENMs with sizes comparable with basic biological components has been used as an argument for the bespoke design of ENMs for medical applications where the materials interact with cells and tissues at a molecular level with a high degree of specificity.[181] In principle, this idea also applies to dental implants incorporating nanotechnology. Table 3 shows some selected examples of the use of ENMs in dental implant applications.

Modifying the surface of Ti implants is one way to improve how an implant interacts with the surrounding tissues. The application of a thin ceramic layer on metallic implants is a popular way to enhance the formation of new bone and avoid adverse inflammatory reactions. The ceramic nanomaterials selected for manufacturing coatings on Ti implants are those that have been classified as bioactive and mainly include HA,[182−184] bioactive glass,[185] and other calcium phosphate compounds.[186,187] Nano-HA is probably the most preferable material used as a coating for Ti, Ti alloy, and stainless steel implants because it is similar to the inorganic component of bone. The application of nano-HA coatings renders the surface of implants biocompatible and encourages an increased cell adherence compared to the metallic surface of uncoated implants. *In vivo* experiments with animal models have suggested that Ti implant surfaces modified with HA NPs show enhanced bone bonding and accelerated new bone formation.[188,189] It has been demonstrated that dental implants coated with HA NPs have better bone-to-implant contact and increased removal torque values compared to the uncoated controls.[190,191] However, the surface roughness and chemistry of implants are not the only factors that determine the biological responses. It has been suggested that particle size and morphology (*e.g*., spherical, rod-shaped, crystals) also play an important role in osteoblast adhesion and their bone-forming capacity.[192,193]

Implants coated with 20−100 nm calcium phosphate (CaP) nanocrystals have demonstrated similar enhanced osseointegrative behavior *in vivo*.[194,195] *In vitro* studies showed that osteoblasts (but not stem cells) had better proliferation on nano-CaP-impregnated Ti implants compared to untreated controls.[196] However, both cell types demonstrated higher differentiation activity on surface-modified specimens. Alumina is another nanoceramic candidate with promising osseointegrative properties. Webster *et al*. reported increased

osteoblast proliferation and adhesion on substrates made of nanosized alumina (24 nm).[197] Alumina nanofibers (2 nm in diameter, 50 nm long) have also been found to encourage osteoblast differentiation and calcium deposition.[198] Yang *et al*. found that smaller particles of nanodiamonds promoted osteoblast adhesion and proliferation more compared to larger particles.[199] This latter finding could be the basis for manufacturing coatings with variable particle sizes to control the degree of bone apposition and favor bone growth at specific anatomical locations. Other types of NPs, such as yttrium-stabilized zirconia and CNT-CaP NPs (Table 3), have also been investigated as means to reinforce Ti alloy and polymer-based implants, respectively.[189,200]

Numerous *in vivo* and *in vitro* studies have suggested that nanoparticulate coatings render dental implants more biocompatible while facilitating formation of new bone and reducing healing time (Table 3). However, a considerable number of scientific reports have also shown no significant benefits from modifying implant surfaces with NPs. *In vivo* studies comparing blasted/acid-etched Ti endosseous implants (controls) with specimens further subjected to a bioceramic deposition process to form a nano-CaP coating did not indicate any difference in bone bonding or healing between the two groups.[201−203] A possible explanation for these results is that the optimal bone quality of the implant bed overshadowed the superior osseointegrative properties of the CaP-coated specimens. This may suggest that *in vivo* studies selecting healthy bone tissues as implantation sites do not mimic the poor state of bone in edentulous patients.

Despite extensive research, it is still not clear whether the improved properties of the nanocoated implants are derived from the chemistry of the coatings or whether it is due to the change that the coatings introduce to the surface roughness of the implants. Mendes *et al*. argue in favor of the latter suggesting that the improved osseointegration found for implants coated with nanocrystalline CaP arises from the complexity of the resultant surface rather than the CaP chemistry itself.[204] In general, the degree of osseointegration is improved with increased surface roughness;[205] and nanomodified dental implants do have increased surface roughness compared to standard metallic implants with polished surfaces. Consequently, one might argue that the advantage of the NPs deposition on the dental implants surfaces is mainly due to the introduced nanotopography. However, further research is required to either support or reject this hypothesis. It is noteworthy that many studies in the current literature fail to fully characterize the implant surfaces under investigation, and in some cases, scanning electron microscopy (SEM) is the only technique employed to describe these surfaces and compare between them. Thus, future studies should include more advanced surface characterization techniques (*e.g*., 3D measurements for SEM, atomic force microscopy, X-ray photoelectron spectroscopy) to assess the nanostructure of coated implants and provide quantitative data, which then could offer a better understanding on whether the bone response is determined by the surface nanotopography.[206,207] Also, further investigation is needed on how the particle size and morphology affects the host response and ultimately the bone bonding.

Dentifrices and Personal Care Products. The use of dentifrices (toothpastes, tooth powders, mouthwashes, *etc*.) to manage oral health and generally help prevent dental caries is recommended to the public. The use of nanotechnology in these products is of growing commercial interest. In principle, ENMs could be used to aid the mineralization process of the enamel and/or dentine (discussed above by providing HA, fluoride), control microbes, and plaque as part of brushing (*e.g*., antimicrobial ENMs, Table 1), or provide nanoscale minerals to enhance pH control (*e.g*., calcium phosphate). Employing artificial nano-HA in dentifrices, such as toothpastes, to restore the lost mineral content of enamel and dentine has been considered as a sensible strategy.[208−211] Nano-HA has been tested in different forms (spherical, needle-like, crystalline). Lu *et al*. found that nano-HA added in toothpaste not only enhanced the microhardness of enamel and improved remineralization but may also reduce bacterial colonization of the tooth surfaces.[209] Other ENMs that have been suggested to promote enamel and dentine remineralization in experimental studies include nanoparticulate bioactive glass,[212,213] nanosized carbonated apatite alone or in combination with silica,[214,215] nanosized calcium fluoride,[216] carbonate-hydroxyapatite nanocrystals,[217] and nanoprecursors of amorphous calcium phosphates.[100] Logically, these materials might also be included in toothpastes or other commercial dentifrices.

Nonetheless, there are some commercial products where the basis for mode of action has been explained. Casein phosphopeptide (CPP), which is produced from a tryptic digest of casein by aggregation with calcium phosphate and purification by ultrafiltration,[218] carries calcium and phosphate ions bound to it in the form of amorphous calcium phosphate (ACP). The CPP-ACP nanocomplex is commercially known as Recaldent and is available as a product under the brand name GC Tooth Mousse (GC Ltd.) in the form of a topical cream. As a rich source of calcium and phosphate ions, the CPP-ACP nanocomplexes have been suggested to promote enamel remineralization. When in the oral cavity, the CPP-ACP nanocomplexes adhere to the enamel, pellicle, plaque, and soft tissue, delivering calcium and phosphate ions. The free calcium and phosphate ions then enter the enamel rods and reform into apatite crystals, contributing to the teeth remineralization.

The role of nano-HA and other Ca-based NPs has been investigated as a treatment for dentine hypersensitivity by occluding the dentinal tubules.[98,219] Application of 40 nm silica NPs has also been found to form a physical barrier at the entrance of dentinal tubules preventing the movement of the fluid within the tubules, which is the cause of sensitivity problems.[99] Strontium chloride was the first tubule blocking agent to be introduced to the market (as Sensodyne) 50 years ago.[220] However, strontium chloride was incompatible with fluoride and was finally replaced with strontium acetate. Although several studies have shown that 10% strontium chloride dentifrices reduce dentine hypersensitivity,[221−223] Zappa, who summarized the results of clinical studies with strontium chloride toothpastes, concluded that the clinical efficacy of strontium-based products was uncertain.[224] Saliva naturally plugs the dentinal tubules both by transporting calcium and phosphate ions into the openings of the channels and by forming a calcium- and phosphate-rich salivary glycoprotein layer.[225] In an attempt to mimic the natural occlusion mechanism, ProClude (Ortek Therapeutics Inc.) was manufactured. ProClude consists of arginine (an amino acid that is positively charged at physiological pH), bicarbonate (a pH buffer), and calcium carbonate (as a source of calcium). Arginine binds to the surface of calcium carbonate and, in the form of positively charged agglomerates, adheres to the negatively charged dentine surface and tubules.[226] Colgate developed the arginine technology (Pro-Argin) further by adding fluoride.[227] However, it has to be noted that a number of studies have shown that brushing with toothpastes designed for sensitive teeth has an adverse effect causing dentine erosion and the tubules to open rather than resolving the problem.[228] Clearly, there is an emerging market for the use of nanotechnology in dental healthcare products, and like other ENMs applications in the food or personal care sectors, the safety and efficacy of these products need to be proven, as well as improved product labeling to give clarity on which products actually contain natural or ENMs (see below).

SAFETY OF ENGINEERED NANOMATERIALS USED IN DENTISTRY

The Safety of Patients. The current regulatory procedures for approving new medicines and medical devices and how they apply to ENMs has recently been discussed,[158] as well as considerations for occupational health.[21,229] Briefly, the overarching process of conducting a clinical trial with a medicine intended for human use is covered by the Clinical Trials Directive (Directive 2001/20/EC), which sets out the implementation of good clinical practice for such trials and various codes relating to medicinal products for humans (*e.g.*, Directive 2004/27/EC). In addition, regulation EC number 726/2004 lays down the procedure for the authorization and supervision of medicinal products, and this involved establishing the European Medicines Agency with some oversight of national level authorities within Europe (Regulation (EC) No 26/2004). Juillerat-Jeanneret *et al*. argue that from a legal and regulatory perspective that these regulations apply equally to nanomedicines, as the fundamental purpose of the regulations is the same for all medicines.[158] Outside the European Union, regulations are often established at national level. For example, in the United States the Food and Drug Administration (FDA) provides federal regulations on the safety of medicines (*e.g.*, Federal Regulations 21). The founding principles behind regulation include demonstrating that the new product is effective for its intended clinical use, or more effective than an existing product, and it must be safe.[158] In the case of dentistry, Annex I of the Medical Devices Directive 93/42/EC identifies some legal requirements on the use of devices that would include dentures and various dental implants, whether or not they contained ENMs. The multivariate use of different ENMs in composites, or to restore dentine, presents some complexity for the regulations since one of the drivers is the intended use of the new substance. For example, the use of Ag NPs as an antibacterial in a composite might be regarded as a medicine, while the inclusion of (for example) CNTs or HA for mechanical properties might fall under the medical devices regulations. Some clarity on these points is needed from governments and regulatory authorities, but it would seem sensible for commercial companies seeking product approval to be guided by the main intended use of the whole product as a starting point.

In essence, risk is a function of exposure and hazard (toxicity), and both aspects are considered in risk assessments for ENMs.[21] For patients the exposure is defined by the intended treatment, the physical form, and concentrations of the ENMs in the therapeutic agent or medical device. Since the intended treatment (exposure) is usually known from the outset, although some investigations of erosion and bioavailability of ENMs from dental materials may be needed, the focus is mainly on hazard assessment. The regulations for toxicity testing also require that the route of uptake, frequency of dosing, formulation, concentration, and administration site must be related to the expected use in humans. Consequently, for medicines used in dentistry, oral toxicity tests on animal models will be relevant; as well as toxicity data on the tissues relevant to the oral cavity.

There are several theoretical routes of exposure for dental patients. These include (i) accidental or incidental ingestion of the nanocontaining dental material during or after treatment; (ii) the generation of aerosols during dental treatment that might present a respiratory

hazard to the patient (*e.g.*, aerosols from drilling into a nanocomposite during a dental repair); (iii) systemic toxicity from any ingested or inhaled ENMs; (iv) direct toxicity to the cells/tissue of the oral cavity.

The ingestion and subsequent systemic hazard from oral exposure to ENMs has been studied in rodents (TiO_2;[230,231] Cu NPs;[232] Ag NPs[19]) and fish (TiO_2;[233] C_{60} and CNTs[234]), as well as *in vitro* using the Caco-2 intestinal cell line[235,236] or isolated perfused intestines.[35] Selected examples of oral toxicity studies with different models are summarized in Table 5. It is clear that some pristine (unmodified) ENMs can be absorbed across the vertebrate gut from an ingested food matrix (*e.g.*, TiO_2[233]), and although for metal-containing ENMs the bioavailability may only be a few percent of the dose, this is not dissimilar to traditional dissolved metal of concern like mercury.[233] However, most oral toxicity studies on animal models have used gut gavage,[232] and there is some concern that ENMs introduced to the gut via salines may have a higher bioavailability than those in a food or dental material matrix. Nonetheless, the use of physiological saline would also be relevant to dental practice.

In vivo studies on rodents show that at least total metal concentrations in the internal organs from exposure to metal-containing ENMs can increase, and this may also lead to organ pathology (Table 5). For example, Wang *et al*. found pathology in liver and kidney of mice after single oral gavage of TiO_2 NPs (25 or 80 nm).[231] There is also at least one report of argyria in humans after chronic ingestion of colloidal silver solution, indicating that silver from nanosilver can be absorbed.[237] However, there is controversy over whether intact particles are absorbed across the gut epithelium. Gitrowski *et al*. recently demonstrated endocytosis of intact TiO_2 NPs by Caco-2 cells.[236] Interestingly, the uptake mechanism was sensitive to endocytosis inhibitors such as nystatin and was also dependent on the crystal structure of the material; indicating that shape/crystal form is also an important aspect of the oral hazard.

The hazard from dental materials must be taken in context with these studies on oral toxicity to animals, and other oral hazards outside of dentistry for the patient as a member of the public. For example, there is a potential dietary exposure risk from food and personal care products containing ENMs.[10,12,238] In addition, the mucociliary escalator in the lung may clear ultrafine particles (*e.g.*, from air pollution) from the airway, which are then subsequently ingested. The relative oral exposure from ENMs during intermittent dental work may be small compared to the potential long-term exposure via the food. For example, Weir *et al*. estimate ingestion of about 1−3 mg of TiO_2 kg body weight^{-1} day^{-1}, with about a third of the material being at the nanoscale.[12] A patient would therefore need to ingest grams of TiO_2 ENM on a visit to the dentist in order to achieve the same annual dose as might be incidentally achieved from food products.

However, the toxicity data in the public domain on ENMs used specifically in dental applications is sparse, with no information on oral toxicity from dental materials, biomaterials, or implants containing ENMs in animal models or patients. As a rule, dental materials for permanent restorations are designed to be inert and chemically stable in the oral environment. However, there has always been a concern that leaching of toxic compounds may occur either as a result of material instability or degradation, or due to inappropriate application or preparation of the dental material by the clinician. Metal release from dental materials is not uncommon (*e.g.*, amalgams, metal alloys[239]), but the reported elemental release is usually negligible or comparable to that of food and drink intake. The release of chemical substances leaching from resin composites[240,241] and endodontic sealers[242,243] has also been confirmed; raising the concern that patients are unnecessarily exposed to potentially toxic chemicals during and after treatment. However, similar information for dental materials containing ENMs is lacking.

There is also a concern of direct contact toxicity from the ENM with the cells and tissues of the oral cavity. The oral epithelium is mostly nonkeratinized stratified squamous epithelium, with the exception of gingiva, hard palate, and dorsal surface of the tongue. The epithelium acts with saliva to form a protective mucous barrier. The salivary film covering the oral cavity has an estimated thickness of 70−100 μm,[244] whereas the thickness of the nonkeratinized squamous epithelium varies between 500 and 800 μm;[245] the latter being thicker than the epithelium of the esophagus (300−500 μm[246]) or the intestines (20−25 μm[247]). It therefore might be argued that the oral cavity is a better barrier than, for example, the more permeable intestine, but this notion derived from the transport of solutes across epithelia has yet to be verified with experimental data for ENMs.[248] It seems likely that some types of ENMs will become trapped in the mucous secretion of the saliva by steric hindrance (discussed above), but nanomedicines are being engineered to cross mucous barriers (*e.g.*, to improve drug delivery[249]), and it is possible that such traits will be useful in dentistry (*e.g.*, delivery of antimicrobials, anesthetics, *etc.*). However, there is a concern that some ENMs are immunogenic[250] and would induce a hypersensitivity reaction or inflammation in a vulnerable patient. This risk may be present with traditional medicines and medical devices, and whether the risk would be greater for an ENM in the oral cavity is unknown.

Occupation Exposure of the Practitioner. The occupational health of the practitioner should also be considered in the context of routes of exposure. For health and safety in the workplace, safe systems of work are

aimed at preventing exposure so that there is a negligible risk. This approach also applies to ENMs,[20,21,251] although in practice employers do show some uncertainty about what might be nanospecific in the governance of health and safety.[252] Potential exposure of the practitioner could arise from incidental ingestion or dermal contact. However, the clinical practice of wearing surgical gloves and not eating or drinking while treating patients should minimize these exposure routes as they would with other substances.

Exposure to aerosols of dental materials containing ENMs has not been quantified in a workplace scenario, and there is a theoretical exposure from activities such as drilling or filing into a restoration that already contains ENMs. There are exposure limits set for dusts and powders that might create an aerosol in the workplace (*e.g.*, 10 mg m^{-3} for an 8 h exposure to dust generally in the U.K.), and reports from various health and safety agencies indicate exposures of a few mg m^{-3} or less to workers in ENM manufacturing plants.[253] The exposure risk to dentists working with only a few grams of dental material at a time is likely, therefore, to be much less. Interestingly, studies on abrasion/sanding of industrial coatings and composites find mainly negligible (not detectable) or low releases of free ENMs.[254] This might imply that a similar activity by a dentist such as abrading/shaping a dental composite might be low risk. However, distance from the point source of the exposure is also critical, and in dentistry, the practitioner is inevitably very close to the patient. Clearly, further research is needed on workplace exposure to ENMs in dentistry.

CONCLUSIONS AND RECOMMENDATIONS

There appears to be many potential benefits to patient outcome from using nanotechnology in dentistry. The benefits include new materials for preventative health care using dentifrices that are either antimicrobial and/or have some restorative properties for the enamel and dentine. The use of ENMs to enhance the mechanical and physiological functions of the tooth via new nanofillers and composites should provide an enhanced capability for some areas of restorative dentistry. The use of ENMs to improve osseointegration, infection control, and biocompatibility of dental implants may reduce the rejection rates in some invasive procedures. There are also completely new frontiers in dental treatment such as the use of ENMs to control and direct pulp stem cells in order to regenerate the tooth.

These potential benefits should be balanced against the risks. For the patient the exposure to ENMs will be controlled by the planned dental treatment, and thus, the main concern is on the hazard of the ENMs in dental materials. The data so far indicates that oral toxicity for ENMs is low, but some ENMs are translocated across the gut to cause systemic disturbances, perhaps with organ pathology. However, the matrix in which the ENM is incorporated will be important, and oral toxicity studies have yet to be done with dental materials containing EMNs. Overall, however, the information so far indicates that the oral hazard is low or manageable and should not be a barrier to the safe innovation of nanotechnology in dentistry. The safety assessment processes in place for medicines and medical devices remain robust, and although individual toxicity tests may need modifications to work well with ENMs, the overall safety strategy is appropriate. Nonetheless, there are some improvements in health and safety that can be made. For example, better guidance to practitioners on nanoincorporated products with respect to patient safety and occupational health. For the public and patients, the nanospecific labeling on the many personal care products in dentistry could be improved to clearly identify the nanoingredient(s). Thus, giving clarity on whether a product actually contains an ENM and what the proposed mode of action or benefit of the new product might be to the consumer.

Research Recommendations and Data Gaps. Although the potential benefits appear to outweigh the risks associated with using ENMs in dentistry, there are still several areas where knowledge can be improved. These include:

(i) Specific research to understand how the protein corona is formed on ENMs in saliva, and how the ENM might change the bioavailability of active ingredients in the saliva. It is also unclear how or if ENMs alter the secretory functions of the salivary glands.

(ii) Research on clinically relevant biofilms. Although there is some understanding of laboratory cultures of microbes and ecologically relevant biofilms, in contrast, biofilms in/on the human body are poorly understood with respect to ENMs. Some targeted research on the oral cavity biofilm is needed to underpin the role of ENMs in drug delivery, antimicrobial functions, and on penetration to the dentine surface.

(iii) Mechanistic investigations on how ENMs strengthen the tooth structure (enamel, dentine, pulp, and cementum) and further exploration of adding physiological function to nanoenhanced dental materials. The use of second and third generation ENMs with complex three-dimensional structures rather than particles needs to be explored for its mechanical properties in dental applications.

(iv) The use of ENMs in dental therapeutics for drug delivery and to provide growth factors involved in tissue regeneration or stem cell treatments is worthy of more investigation with respect to both efficacy and safety.

(v) New dentifrices containing ENMs offer the chance of preventative dentistry and better

public health, but consumer choice is important. Research on the composition of existing products and product labeling are part of improving consumer confidence in using commercial products containing nanotechnology.

Conflict of Interest: The authors declare no competing financial interest.

REFERENCES AND NOTES

1. Sekiguchi, Y.; Yao, Y.; Ohko, Y.; Tanaka, K.; Ishido, T.; Fujishima, A.; Kubota, Y. Self-sterilizing Catheters with Titanium Dioxide Photocatalyst Thin Films for Clean Intermittent Catheterization: Basis and Study of Clinical Use. *Int. J. Urol.* **2007**, *14*, 426–430.
2. Kumar, P. T.; Lakshmanan, V. K.; Biswas, R.; Nair, S. V.; Jayakumar, R. Synthesis and Biological Evaluation of Chitin Hydrogel/Nano ZnO Composite Bandage As Antibacterial Wound Dressing. *J. Biomed. Nanotechnol.* **2012**, *8*, 891–900.
3. Zhang, L.; Chan, J. M.; Gu, F. X.; Rhee, J. W.; Wang, A. Z.; Radovic-Moreno, A. F.; Alexis, F.; Langer, R.; Farokhzad, O. C. Self-Assembled Lipid-Polymer Hybrid Nanoparticles: A Robust Drug Delivery Platform. *ACS Nano* **2008**, *2*, 1696–1702.
4. Namiki, Y.; Fuchigami, T.; Tada, N.; Kawamura, R.; Matsunuma, S.; Kitamoto, Y.; Nakagawa, M. Nanomedicine for Cancer: Lipid-Based Nanostructures for Drug Delivery and Monitoring. *Acc. Chem. Res.* **2011**, *44*, 1080–1093.
5. Pablico-Lansigan, M. H.; Situ, S. F.; Samia, A. C. Magnetic Particle Imaging: Advancements and Perspectives for Real-Time *in Vivo* Monitoring and Image-Guided Therapy. *Nanoscale* **2013**, *5*, 4040–4055.
6. Allaker, R. P. The Use of Nanoparticles to Control Oral Biofilm Formation. *J. Dent. Res.* **2010**, *89*, 1175–1186.
7. Hernández, d. l. F.; Javier, M. A. A. P.; Valenzuela, M. C. S. Use of New Technologies in Dentistry. *Rev. Odontol. Mex.* **2011**, *15*, 158–163.
8. Gupta, S.; Rakesh, K.; Gupta, O. P.; Khanna, S.; Purwar, A.; Verma, Y. Role of Nanotechnology and Nanoparticles in Dentistry: A Review. *Int. J. Res. Dev.* **2013**, *1*, 95–102.
9. Chaudhry, Q.; Scotter, M.; Blackburn, J.; Ross, B.; Boxall, A.; Castle, L.; Aitken, R.; Watkins, R. Applications and Implications of Nanotechnologies for the Food Sector. *Food Addit. Contam.* **2008**, *25*, 241–258.
10. Tiede, K.; Boxall, A. B.; Tear, S. P.; Lewis, J.; David, H.; Hassellov, M. Detection and Characterization of Engineered Nanoparticles in Food and the Environment. *Food Addit. Contam.* **2008**, *25*, 795–821.
11. Aitken, R. J.; Chaudhry, M. Q.; Boxall, A. B.; Hull, M. Manufacture and Use of Nanomaterials: Current Status in the UK and Global Trends. *Occup. Med.* **2006**, *56*, 300–306.
12. Weir, A.; Westerhoff, P.; Fabricius, L.; Hristovski, K.; von Goetz, N. Titanium Dioxide Nanoparticles in Food and Personal Care Products. *Environ. Sci. Technol.* **2012**, *46*, 2242–2250.
13. Powell, J. J.; Faria, N.; Thomas-McKay, E.; Pele, L. C. Origin and Fate of Dietary Nanoparticles and Microparticles in the Gastrointestinal Tract. *J. Autoimmun.* **2010**, *34*, 226–233.
14. Lomer, M. C.; Thompson, R. P.; Commisso, J.; Keen, C. L.; Powell, J. J. Determination of Titanium Dioxide in Foods Using Inductively Coupled Plasma Optical Emission Spectrometry. *Analyst* **2000**, *125*, 2339–2343.
15. Schrand, A. M.; Rahman, M. F.; Hussain, S. M.; Schlager, J. J.; Smith, D. A.; Syed, A. F. Metal-Based Nanoparticles and Their Toxicity Assessment. *Wiley Interdiscip. Rev. Nanomed. Nanobiotechnol.* **2010**, *2*, 544–568.
16. Iavicoli, I.; Leso, V.; Fontana, L.; Bergamaschi, A. Toxicological Effects of Titanium Dioxide Nanoparticles: A Review of *in Vitro* Mammalian Studies. *Eur. Rev. Med. Pharmacol. Sci.* **2011**, *15*, 481–508.
17. Mitsiadis, T. A.; Woloszyk, A.; Jimenez-Rojo, L. Nanodentistry: Combining Nanostructured Materials and Stem Cells for Dental Tissue Regeneration. *Nanomedicine* **2012**, *7*, 1743–1753.
18. Sharma, V.; Singh, P.; Pandey, A. K.; Dhawan, A. Induction of Oxidative Stress, DNA Damage and Apoptosis in Mouse Liver after Sub-Acute Oral Exposure to Zinc Oxide Nanoparticles. *Mutat. Res.* **2012**, *745*, 84–91.
19. van der Zande, M.; Vandebriel, R. J.; van Doren, E.; Kramer, E.; Herrera Rivera, Z.; Serrano-Rojero, C. S.; Gremmer, E. R.; Mast, J.; Peters, R. J.; Hollman, P. C.; et al. Distribution, Elimination, and Toxicity of Silver Nanoparticles and Silver Ions in Rats after 28-Day Oral Exposure. *ACS Nano* **2012**, *6*, 7427–7442.
20. Handy, R. D.; Shaw, B. J. Toxic Effects of Nanoparticles and Nanomaterials: Implications for Public Health, Risk Assessment and the Public Perception of Nanotechnology. *Health Risk Soc.* **2007**, *9*, 125–144.
21. Rocks, S. A.; Pollard, S. J.; Dorey, R. A.; Harrison, P. T. C.; Levy, L. S.; Handy, R. D.; Garrod, J. F.; Owen, R. Risk Assessment of Manufactured Nanomaterials. In *Environmental and Human Health Impacts of Nanotechnology*; Lead, J. R., Smith, E., Eds.; Blackwell Publishing Ltd: New York, 2009; pp 389−421.
22. Donaldson, K.; Brown, D.; Clouter, A.; Duffin, R.; MacNee, W.; Renwick, L.; Tran, L.; Stone, V. The Pulmonary Toxicology of Ultrafine Particles. *J. Aerosol Med.* **2002**, *15*, 213–220.
23. Donaldson, K.; Aitken, R.; Tran, L.; Stone, V.; Duffin, R.; Forrest, G.; Alexander, A. Carbon Nanotubes: A Review of Their Properties in Relation to Pulmonary Toxicology and Workplace Safety. *Toxicol. Sci.* **2006**, *92*, 5–22.
24. Helland, A.; Wick, P.; Koehler, A.; Schmid, K.; Som, C. Reviewing the Environmental and Human Health Knowledge Base of Carbon Nanotubes. *Environ. Health Perspect.* **2007**, *115*, 1125–1131.
25. Warheit, D. B.; Sayes, C. M.; Reed, K. L.; Swain, K. A. Health Effects Related to Nanoparticle Exposures: Environmental, Health and Safety Considerations for Assessing Hazards and Risks. *Pharmacol. Ther.* **2008**, *120*, 35–42.
26. Poland, C. A.; Duffin, R.; Kinloch, I.; Maynard, A.; Wallace, W. A.; Seaton, A.; Stone, V.; Brown, S.; Macnee, W.; Donaldson, K. Carbon Nanotubes Introduced into the Abdominal Cavity of Mice Show Asbestos-Like Pathogenicity in a Pilot Study. *Nat. Nanotechnol.* **2008**, *3*, 423–428.
27. Pedersen, A. M.; Bardow, A.; Jensen, S. B.; Nauntofte, B. Saliva and Gastrointestinal Functions of Taste, Mastication, Swallowing and Digestion. *Oral Dis.* **2002**, *8*, 117–129.
28. Edgar, W. M.; Higham, S. M.; Manning, R. H. Saliva Stimulation and Caries Prevention. *Adv. Dent. Res.* **1994**, *8*, 239–245.
29. Stookey, G. K. The Effect of Saliva on Dental Caries. *J. Am. Dent. Assoc.* **2008**, *139*, 11–17.
30. Lead, J. R.; Wilkinson, K. J. Aquatic Colloids and Nanoparticles: Current Knowledge and Future Trends. *Environ. Chem.* **2006**, *3*, 159–171.
31. Handy, R. D.; von der Kammer, F.; Lead, J. R.; Hassellov, M.; Owen, R.; Crane, M. The Ecotoxicology and Chemistry of Manufactured Nanoparticles. *Ecotoxicology* **2008**, *17*, 287–314.
32. Ju-Nam, Y.; Lead, J. R. Manufactured nanoparticles: An Overview of Their Chemistry, Interactions and Potential Environmental Implications. *Sci. Total Environ.* **2008**, *400*, 396–414.
33. von der Kammer, F.; Ferguson, P. L.; Holden, P. A.; Masion, A.; Rogers, K. R.; Klaine, S. J.; Koelmans, A. A.; Horne, N.; Unrine, J. M. Analysis of Engineered Nanomaterials in Complex Matrices (Environment and Biota): General Considerations and Conceptual Case Studies. *Environ. Toxicol. Chem.* **2012**, *31*, 32–49.
34. Whelton, H. Introduction: The Anatomy and Physiology of the Salivary Glands. In *Saliva and Oral Health*, third ed.; Edgar, M. C. D., O'Mullane, D., Eds.; British Dental Journal: London, 2004; pp 1−16.

35. Al-Jubory, A. R.; Handy, R. D. Uptake of Titanium from TiO_2 Nanoparticle Exposure in the Isolated Perfused Intestine of Rainbow Trout: Nystatin, Vanadate and Novel CO_2-Sensitive Components. *Nanotoxicology* **2013**, *7*, 1282–1301.
36. Besinis, A.; De Peralta, T.; Handy, R. D. Inhibition of Biofilm Formation and Antibacterial Properties of a Silver Nano-Coating on Human Dentine. *Nanotoxicology* **2014**, *8*, 745–754.
37. Handy, R. D.; Maunder, R. J. The Biological Roles of Mucus: Importance for Osmoregulation and Osmoregulatory Disorders of Fish Health. In *Osmoregulation and Ion Transport: Integrating Physiological, Molecular and Environmental Aspects. Essential Reviews in Experimental Biology*; Handy, R. D., Bury, N. R., Eds.; Society for Experimental Biology Press: London, 2009; pp 203−235.
38. Dawes, C. Estimates, from Salivary Analyses, of the Turnover Time of the Oral Mucosal Epithelium in Humans and the Number of Bacteria in an Edentulous Mouth. *Arch. Oral Biol.* **2003**, *48*, 329–336.
39. Proctor, G. B.; Carpenter, G. H. Regulation of Salivary Gland Function by Autonomic Nerves. *Auton. Neurosci.* **2007**, *133*, 3–18.
40. Windeatt, K. M.; Handy, R. D. Effect of Nanomaterials on the Compound Action Potential of the Shore Crab, *Carcinus Maenas*. *Nanotoxicology* **2013**, *7*, 378–388.
41. Ruh, H.; Kuhl, B.; Brenner-Weiss, G.; Hopf, C.; Diabate, S.; Weiss, C. Identification of Serum Proteins Bound to Industrial Nanomaterials. *Toxicol. Lett.* **2012**, *208*, 41–50.
42. Xu, Z.; Liu, X. W.; Ma, Y. S.; Gao, H. W. Interaction of Nano-TiO2 with Lysozyme: Insights into the Enzyme Toxicity of Nanosized Particles. *Environ. Sci. Pollut. Res. Int.* **2010**, *17*, 798–806.
43. Song, Y.; Qu, K.; Zhao, C.; Ren, J.; Qu, X. Graphene Oxide: Intrinsic Peroxidase Catalytic Activity and Its Application to Glucose Detection. *Adv. Mater.* **2010**, *22*, 2206–2210.
44. Schenkels, L. C.; Veerman, E. C.; Nieuw Amerongen, A. V. Biochemical Composition of Human Saliva in Relation to Other Mucosal Fluids. *Crit. Rev. Oral Biol. Med.* **1995**, *6*, 161–175.
45. Hannig, M. Ultrastructural Investigation of Pellicle Morphogenesis at Two Different Intraoral Sites During a 24-h Period. *Clin. Oral Invest.* **1999**, *3*, 88–95.
46. Levine, M. J.; Tabak, L. A.; Reddy, M.; Mandel, I. D. Nature of Salivary Pellicles in Microbial Adherence: Role of Salivary Mucins. In *Molecular Basis of Oral Microbial Adhesion*; Mergenhagen, S. E., Rosan, B., Eds.; American Society for Microbiology: Washington, D.C., 1985; pp 125−130.
47. Yao, Y.; Grogan, J.; Zehnder, M.; Lendenmann, U.; Nam, B.; Wu, Z.; Costello, C. E.; Oppenheim, F. G. Compositional Analysis of Human Acquired Enamel Pellicle by Mass Spectrometry. *Arch. Oral Biol.* **2001**, *46*, 293–303.
48. Zahradnik, R. T.; Propas, D.; Moreno, E. C. *In Vitro* Enamel Demineralization by *Streptococcus Mutans* in the Presence of Salivary Pellicles. *J. Dent. Res.* **1977**, *56*, 1107–1110.
49. Hannig, M.; Balz, M. Protective Properties of Salivary Pellicles from Two Different Intraoral Sites on Enamel Erosion. *Caries Res.* **2001**, *35*, 142–148.
50. Hara, A. T.; Ando, M.; Gonzalez-Cabezas, C.; Cury, J. A.; Serra, M. C.; Zero, D. T. Protective Effect of the Dental Pellicle Against Erosive Challenges *in Situ*. *J. Dent. Res.* **2006**, *85*, 612–616.
51. Lendenmann, U.; Grogan, J.; Oppenheim, F. G. Saliva and Dental Pellicle - A Review. *Adv. Dent. Res.* **2000**, *14*, 22–28.
52. Rolla, G.; Rykke, M. Evidence for Presence of Micelle-Like Protein Globules in Human Saliva. *Colloid Surf., B* **1994**, *3*, 177–182.
53. Cedervall, T.; Lynch, I.; Lindman, S.; Berggard, T.; Thulin, E.; Nilsson, H.; Dawson, K. A.; Linse, S. Understanding the Nanoparticle-Protein Corona Using Methods to Quantify Exchange Rates and Affinities of Proteins for Nanoparticles. *Proc. Natl. Acad. Sci. U.S.A.* **2007**, *104*, 2050–2055.
54. Lundqvist, M.; Stigler, J.; Elia, G.; Lynch, I.; Cedervall, T.; Dawson, K. A. Nanoparticle Size and Surface Properties Determine the Protein Corona with Possible Implications for Biological Impacts. *Proc. Natl. Acad. Sci. U.S.A.* **2008**, *105*, 14265–14270.
55. Hellstrand, E.; Lynch, I.; Andersson, A.; Drakenberg, T.; Dahlback, B.; Dawson, K. A.; Linse, S.; Cedervall, T. Complete High-Density Lipoproteins in Nanoparticle Corona. *FEBS J.* **2009**, *276*, 3372–3381.
56. Rezwan, K.; Studart, A. R.; Voros, J.; Gauckler, L. J. Change of Zeta Potential of Biocompatible Colloidal Oxide Particles upon Adsorption of Bovine Serum Albumin and Lysozyme. *J. Phys. Chem. B* **2005**, *109*, 14469–14474.
57. Hernandez-Sierra, J. F.; Ruiz, F.; Pena, D. C.; Martinez-Gutierrez, F.; Martinez, A. E.; Guillen Ade, J.; Tapia-Perez, H.; Castanon, G. M. The Antimicrobial Sensitivity of *Streptococcus Mutans* to Nanoparticles of Silver, Zinc Oxide, and Gold. *Nanomedicine* **2008**, *4*, 237–240.
58. Besinis, A.; De Peralta, T.; Handy, R. D. The Antibacterial Effects of Silver, Titanium Dioxide and Silica Dioxide Nanoparticles Compared to the Dental Disinfectant Chlorhexidine on *Streptococcus Mutans* Using a Suite of Bioassays. *Nanotoxicology* **2014**, *8*, 1–16.
59. Bradford, A.; Handy, R. D.; Readman, J. W.; Atfield, A.; Muhling, M. Impact of Silver Nanoparticle Contamination on the Genetic Diversity of Natural Bacterial Assemblages in Estuarine Sediments. *Environ. Sci. Technol.* **2009**, *43*, 4530–4536.
60. Merrifield, D. L.; Shaw, B. J.; Harper, G. M.; Saoud, I. P.; Davies, S. J.; Handy, R. D.; Henry, T. B. Ingestion of Metal-Nanoparticle Contaminated Food Disrupts Endogenous Microbiota in Zebrafish (*Danio Rerio*). *Environ. Pollut.* **2013**, *174*, 157–163.
61. Handy, R. D.; van den Brink, N.; Chappell, M.; Muhling, M.; Behra, R.; Dusinska, M.; Simpson, P.; Ahtiainen, J.; Jha, A. N.; Seiter, J.; et al. Practical Considerations for Conducting Ecotoxicity Test Methods with Manufactured Nanomaterials: What Have We Learnt So Far? *Ecotoxicology* **2012**, *21*, 933–972.
62. Einstein, A. *Investigations on the Theory of the Brownian Movement*; Dover Publications: New York, 1956.
63. Stoodley, P.; Boyle, J. D.; Lappin-Scott, H. In *Dental Plaque Revisited*; Newman, H. N., Wilson, M., Eds.; Bioline: Cardiff, U.K., 1999; pp 63−72.
64. Thurnheer, T.; Gmur, R.; Shapiro, S.; Guggenheim, B. Mass Transport of Macromolecules within an *in Vitro* Model of Supragingival Plaque. *Appl. Environ. Microbiol.* **2003**, *69*, 1702–1709.
65. Handy, R. D.; Eddy, F. B. In *Physicochemical Kinetics and Transport at Chemical-Biological Interphases*; van Leeuwen, H. P., Köster, W., Eds.; John Wiley: Chichester, U.K., 2004; pp 337−356.
66. Jiang, J.; Oberdörster, G.; Biswas, P. Characterization of Size, Surface Charge, and Agglomeration State of Nanoparticle Dispersions for Toxicological Studies. *J. Nanopart. Res.* **2009**, *11*, 77–89.
67. Gebauer, J. S.; Treuel, L. Influence of Individual Ionic Components on the Agglomeration Kinetics of Silver Nanoparticles. *J. Colloid Interface Sci.* **2011**, *354*, 546–554.
68. Jiang, X.; Weise, S.; Hafner, M.; Rocker, C.; Zhang, F.; Parak, W. J.; Nienhaus, G. U. Quantitative Analysis of the Protein Corona on FePt Nanoparticles Formed by Transferrin Binding. *J. R. Soc. Interface* **2010**, *7*, 5–13.
69. Maiorano, G.; Sabella, S.; Sorce, B.; Brunetti, V.; Malvindi, M. A.; Cingolani, R.; Pompa, P. P. Effects of Cell Culture Media on the Dynamic Formation of Protein-Nanoparticle Complexes and Influence on the Cellular Response. *ACS Nano* **2010**, *4*, 7481–7491.
70. Kralj, S.; Rojnik, M.; Romih, R.; Jagodic, M.; Kos, J.; Makovec, D. Effect of Surface Charge on the Cellular Uptake of Fluorescent Magnetic Nanoparticles. *J. Nanopart. Res.* **2012**, *14*, 1151–1164.
71. Petri-Fink, A.; Steitz, B.; Finka, A.; Salaklang, J.; Hofmann, H. Effect of Cell Media on Polymer Coated Superparamagnetic Iron Oxide Nanoparticles (SPIONs): Colloidal Stability, Cytotoxicity, and Cellular Uptake Studies. *Eur. J. Pharm. Biopharm.* **2008**, *68*, 129–137.

72. Sharma, A. K.; Schmidt, B.; Frandsen, H.; Jacobsen, N. R.; Larsen, E. H.; Binderup, M. L. Genotoxicity of Unmodified and Organo-Modified Montmorillonite. *Mutat. Res.* **2010**, *700*, 18–25.
73. Lordan, S.; Higginbotham, C. L. Effect of Serum Concentration on the Cytotoxicity of Clay Particles. *Cell Biol. Int.* **2012**, *36*, 57–61.
74. Aubin-Tam, M. E.; Hamad-Schifferli, K. Gold Nanoparticle-Cytochrome C Complexes: the Effect of Nanoparticle Ligand Charge on Protein Structure. *Langmuir* **2005**, *21*, 12080–12084.
75. Bloom, W.; Fawcett, D. W. *A Textbook of Histology*; W. B. Saunders: Philadelphia, PA, 1968.
76. Park, S.; Wang, D. H.; Zhang, D.; Romberg, E.; Arola, D. Mechanical Properties of Human Enamel as a Function of Age and Location in the Tooth. *J. Mater. Sci. Mater. Med.* **2008**, *19*, 2317–2324.
77. Grine, F. E.; Stevens, N. J.; Jungers, W. L. An Evaluation of Dental Radiograph Accuracy in the Measurement of Enamel Thickness. *Arch. Oral Biol.* **2001**, *46*, 1117–1125.
78. Weatherell, J. A. Composition of Dental Enamel. *Br. Med. Bull.* **1975**, *31*, 115–119.
79. Zipkin, I. In *Biological Calcification*; Schraer, H., Ed.; Appleton-Century-Crofts: New York, 1970; pp 69−103.
80. Weatherell, J. A.; Robinson, C. In *Biological Mineralization*, Zipkin, I., Ed.; John Wiley & Sons: New York, 1973; pp 43−74.
81. Piesco, N. P.; Simmelink, J. Histology of Enamel. In *Oral Development and Histology*; Avery, J. K., Ed.; Georg Thieme Verlag: New York, 2002; pp 153−171.
82. Kerebel, B.; Daculsi, G.; Kerebel, L. M. Ultrastructural Studies of Enamel Crystallites. *J. Dent. Res.* **1979**, *58*, 844–851.
83. Diekwisch, T. G.; Berman, B. J.; Gentner, S.; Slavkin, H. C. Initial Enamel Crystals Are Not Spatially Associated with Mineralized Dentine. *Cell Tissue Res.* **1995**, *279*, 149–167.
84. Hoppenbrouwers, P. M.; Scholberg, H. P.; Borggreven, J. M. Measurement of the Permeability of Dental Enamel and Its Variation with Depth Using an Electrochemical Method. *J. Dent. Res.* **1986**, *65*, 154–157.
85. Kwon, S. R.; Wertz, P. W.; Li, Y.; Chan, D. C. Penetration Pattern of Rhodamine Dyes into Enamel and Dentin: Confocal Laser Microscopy Observation. *Int. J. Cosmet. Sci.* **2012**, *34*, 97–101.
86. Ubaldini, A. L.; Baesso, M. L.; Medina Neto, A.; Sato, F.; Bento, A. C.; Pascotto, R. C. Hydrogen Peroxide Diffusion Dynamics in Dental Tissues. *J. Dent. Res.* **2013**, *92*, 661–665.
87. Nguyen, T. T.; Miller, A.; Orellana, M. F. Characterization of the Porosity of Human Dental Enamel and Shear Bond Strength *in Vitro* after Variable Etch Times: Initial Findings Using the BET Method. *Angle Orthod.* **2011**, *81*, 707–715.
88. Li, L.; Pan, H. H.; Tao, J. H.; Xu, X. R.; Mao, C. Y.; Gu, X. H.; Tang, R. K. Repair of Enamel by Using Hdroxyapatite Nanoparticles As the Building Blocks. *J. Mater. Chem.* **2008**, *18*, 4079–4084.
89. Cai, Y.; Tang, R. Calcium Phosphate Nanoparticles in Biomineralization and Biomaterials. *J. Mater. Chem.* **2008**, *18*, 3775–3787.
90. Sasaki, T.; Hohenester, E.; Gohring, W.; Timpl, R. Crystal Structure and Mapping by Site-Directed Mutagenesis of the Collagen-Binding Epitope of an Activated Form of BM-40/SPARC/Osteonectin. *EMBO J.* **1998**, *17*, 1625–1634.
91. Tye, C. E.; Hunter, G. K.; Goldberg, H. A. Identification of the Type I Collagen-Binding Domain of Bone Sialoprotein and Characterization of the Mechanism of Interaction. *J. Biol. Chem.* **2005**, *280*, 13487–13492.
92. Piesco, N. P.; Simmelink, J. Histology of Dentin. In *Oral Development and Histology*; Avery, J. K., Ed.; Georg Thieme Verlag: New York, 2002; pp 172−187.
93. Lees, S. A Model for the Distribution of HAP Crystallites in Bone - An Hypothesis. *Calcified Tissue Int.* **1979**, *27*, 53–56.
94. Lees, S.; Prostak, K. The Locus of Mineral Crystallites in Bone. *Connect. Tissue Res.* **1988**, *18*, 41–54.
95. Marshall, G. W., Jr.; Marshall, S. J.; Kinney, J. H.; Balooch, M. The Dentin Substrate: Structure and Properties Related to Bonding. *J. Dent.* **1997**, *25*, 441–458.
96. Kinney, J. H.; Pople, J. A.; Marshall, G. W.; Marshall, S. J. Collagen Orientation and Crystallite Size in Human Dentin: A Small Angle X-ray Scattering Study. *Calcified Tissue Int.* **2001**, *69*, 31–37.
97. Garberoglio, R.; Brannstrom, M. Scanning Electron Microscopic Investigation of Human Dentinal Tubules. *Arch. Oral Biol.* **1976**, *21*, 355–362.
98. Earl, J. S.; Wood, D. J.; Milne, S. J. Dentine Infiltration a Cure for Sensitive Teeth. *Am. Ceram. Soc. Bull.* **2006**, *85*, 22–25.
99. Earl, J. S.; Wood, D. J.; Milne, S. J. Nanoparticles for Dentine Tubule Infiltration: An *in Vitro* Study. *J. Nanosci. Nanotechnol.* **2009**, *9*, 6668–6674.
100. Tay, F. R.; Pashley, D. H. Guided Tissue remineralization of Partially Demineralised Human Dentine. *Biomaterials* **2008**, *29*, 1127–1137.
101. Besinis, A.; van Noort, R.; Martin, N. Infiltration of Demineralized Dentin with Silica and Hydroxyapatite Nanoparticles. *Dent. Mater.* **2012**, *28*, 1012–1023.
102. van Meerbeek, B.; Dhem, A.; Goret-Nicaise, M.; Braem, M.; Lambrechts, P.; VanHerle, G. Comparative SEM and TEM Examination of the Ultrastructure of the Resin-Dentin Interdiffusion Zone. *J. Dent. Res.* **1993**, *72*, 495–501.
103. Tay, F. R.; Moulding, K. M.; Pashley, D. H. Distribution of Nanofillers from a Simplified-Step Adhesive in Acid-Conditioned Dentin. *J. Adhes. Dent.* **1999**, *1*, 103–117.
104. Besinis, A.; van Noort, R.; Martin, N. Remineralization Potential of Fully Demineralized Dentin Infiltrated with Silica and Hydroxyapatite Nanoparticles. *Dent. Mater.* **2014**, *30*, 249–262.
105. Bosshardt, D. D.; Selvig, K. A. Dental Cementum: The Dynamic Tissue Covering of the Root. *Periodontol. 2000* **1997**, *13*, 41–75.
106. Carvalho, S. M.; Oliveira, A. A.; Jardim, C. A.; Melo, C. B.; Gomes, D. A.; de Fatima Leite, M.; Pereira, M. M. Characterization and Induction of Cementoblast Cell Proliferation by Bioactive Glass Nanoparticles. *J. Tissue Eng. Regen. Med.* **2012**, *6*, 813–21.
107. Chandra, S. *Textbook of Operative Dentistry*; Jaypee Brothers Medical Publishers: New Delhi, India, 2008.
108. Casagrande, L.; Cordeiro, M. M.; Nor, S. A.; Nor, J. E. Dental Pulp Stem Cells in Regenerative Dentistry. *Odontology* **2011**, *99*, 1–7.
109. Wang, J.; Chen, J.; Zhang, K.; Zhao, Y.; Nor, J. E.; Wu, J. TGF-Beta1 Regulates the Invasive and Metastatic Potential of Mucoepidermoid Carcinoma Cells. *J. Oral Pathol. Med.* **2011**, *40*, 762–768.
110. Campos, M. S.; Neiva, K. G.; Meyers, K. A.; Krishnamurthy, S.; Nor, J. E. Endothelial Derived Factors Inhibit Anoikis of Head and Neck Cancer Stem Cells. *Oral Oncol.* **2012**, *48*, 26–32.
111. Olyveira, G. M.; Acasigua, G. A.; Costa, L. M.; Scher, C. R.; Xavier Filho, L.; Pranke, P. H.; Basmaji, P. Human Dental Pulp Stem Cell Behavior Using Natural Nanotolith/Bacterial Cellulose Scaffolds for Regenerative Medicine. *J. Biomed. Nanotechnol.* **2013**, *9*, 1370–1377.
112. Nguyen, D. H.; Martin, J. T. Common Dental Infections in the Primary Care Setting. *Am. Fam. Physician* **2008**, *77*, 797–802.
113. van der Weijden, F.; Slot, D. E. Oral Hygiene in the Prevention of Periodontal Diseases: The Evidence. *Periodontol. 2000* **2011**, *55*, 104–123.
114. Hannig, M.; Joiner, A. The Structure, Function and Properties of the Acquired Pellicle. *Monogr. Oral Sci.* **2006**, *19*, 29–64.
115. Hannig, C.; Hannig, M. The Oral Cavity - A Key System to Understand Substratum-Dependent Bioadhesion on Solid Surfaces in Man. *Clin. Oral Investig.* **2009**, *13*, 123–139.
116. Ashwood, P.; Thompson, R. P.; Powell, J. J. Fine Particles That Adsorb Lipopolysaccharide *via* Bridging Calcium Cations May Mimic Bacterial Pathogenicity Towards Cells. *Exp. Biol. Med.* **2007**, *232*, 107–117.
117. Hannig, C.; Hannig, M. Natural Enamel Wear - A Physiological Source of Hydroxylapatite Nanoparticles for Biofilm Management and Tooth Repair? *Med. Hypotheses* **2010**, *74*, 670–672.

118. O'Sullivan, E. A.; Williams, S. A.; Wakefield, R. C.; Cape, J. E.; Curzon, M. E. Prevalence and Site Characteristics of Dental Caries in Primary Molar Teeth from Prehistoric times to the 18th Century in England. *Caries Res.* **1993**, *27*, 147–153.
119. Tayles, N.; Domett, K.; Nelsen, K. Agriculture and dental caries? The Case of Rice in Prehistoric Southeast Asia. *World Archaeol.* **2000**, *32*, 68–83.
120. Temple, D. H.; Larsen, C. S. Dental Caries Prevalence As Evidence for Agriculture and Subsistence Variation During the Yayoi Period in Prehistoric Japan: Biocultural Interpretations of an Economy in Transition. *Am. J. Phys. Anthropol.* **2007**, *134*, 501–512.
121. Mjor, I. A.; Moorhead, J. E.; Dahl, J. E. Reasons for Replacement of Restorations in Permanent Teeth in General Dental Practice. *Int. Dent. J.* **2000**, *50*, 361–366.
122. Sarrett, D. C. Clinical Challenges and the Relevance of Materials Testing for Posterior Composite Restorations. *Dent. Mater.* **2005**, *21*, 9–20.
123. Bernardo, M.; Luis, H.; Martin, M. D.; Leroux, B. G.; Rue, T.; Leitao, J.; DeRouen, T. A. Survival and Reasons for Failure of Amalgam Versus Composite Posterior Restorations Placed in a Randomized Clinical Trial. *J. Am. Dent. Assoc.* **2007**, *138*, 775–783.
124. Welch, K.; Cai, Y.; Engqvist, H.; Stromme, M. Dental Adhesives with Bioactive and on-Demand Bactericidal Properties. *Dent. Mater.* **2010**, *26*, 491–499.
125. Yip, K. H.; Poon, B. K.; Chu, F. C.; Poon, E. C.; Kong, F. Y.; Smales, R. J. Clinical Evaluation of Packable and Conventional Hybrid Resin-Based Composites for Posterior Restorations in Permanent Teeth: Results at 12 Months. *J. Am. Dent. Assoc.* **2003**, *134*, 1581–1589.
126. Loguercio, A. D.; Reis, A.; Hernandez, P. A.; Macedo, R. P.; Busato, A. L. 3-Year Clinical Evaluation of Posterior Packable Composite Resin Restorations. *J. Oral Rehabil.* **2006**, *33*, 144–151.
127. Sadeghi, M.; Lynch, C. D.; Shahamat, N. Eighteen-Month Clinical Evaluation of Microhybrid, Packable and Nanofilled Resin Composites in Class I Restorations. *J. Oral Rehabil.* **2010**, *37*, 532–537.
128. Attar, N.; Korkmaz, Y. Effect of Two Light-Emitting Diode (LED) and One Halogen Curing Light on the Microleakage of Class V Flowable Composite Restorations. *J. Contemp. Dent. Pract.* **2007**, *8*, 80–88.
129. Sadeghi, M.; Lynch, C. D. The Effect of Flowable Materials on the Microleakage of Class II Composite Restorations That Extend Apical to the Cemento-Enamel Junction. *Oper. Dent.* **2009**, *34*, 306–311.
130. Cox, M.; Chandler, J.; Boyle, A.; Kneller, P.; Haslam, R. Eighteenth and Nineteenth Century Dental Restoration, Treatment and Consequences in a British Nobleman. *Br. Dent. J.* **2000**, *189*, 593–596.
131. Goldberg, M.; Lacerda-Pinheiro, S.; Priam, F.; Jegat, N.; Six, N.; Bonnefoix, M.; Septier, D.; Chaussain-Miller, C.; Veis, A.; Denbesten, P.; et al. Matricellular Molecules and Odontoblast Progenitors As Tools for Dentin Repair and Regeneration. *Clin. Oral Investig.* **2008**, *12*, 109–112.
132. Smith, A. J.; Murray, P. E.; Sloan, A. J.; Matthews, J. B.; Zhao, S. Trans-Dentinal Stimulation of Tertiary Dentinogenesis. *Adv. Dent. Res.* **2001**, *15*, 51–54.
133. Lang, N. P.; Tan, W. C.; Krahenmann, M. A.; Zwahlen, M. A Systematic Review of the Effects of Full-Mouth Debridement with and without Antiseptics in Patients with Chronic Periodontitis. *J. Clin. Periodontol.* **2008**, *35*, 8–21.
134. Gardin, C.; Ferroni, L.; Favero, L.; Stellini, E.; Stomaci, D.; Sivolella, S.; Bressan, E.; Zavan, B. Nanostructured Biomaterials for Tissue Engineered Bone Tissue Reconstruction. *Int. J. Mol. Sci.* **2012**, *13*, 737–757.
135. Al-Hezaimi, K.; Al-Askar, M.; Al-Rasheed, A. Characteristics of Newly-Formed Cementum Following Emdogain Application. *Int. J. Oral Sci.* **2011**, *3*, 21–26.
136. Melo, M. A.; Guedes, S. F.; Xu, H. H.; Rodrigues, L. K. Nanotechnology-Based Restorative Materials for Dental Caries Management. *Trends Biotechnol.* **2013**, *31*, 459–467.
137. Ahn, S. J.; Lee, S. J.; Kook, J. K.; Lim, B. S. Experimental Antimicrobial Orthodontic Adhesives Using Nanofillers and Silver Nanoparticles. *Dent. Mater.* **2009**, *25*, 206–213.
138. Huang, H.-L.; Chang, Y.-Y.; Lai, M.-C.; Lin, C.-R.; Lai, C.-H.; Shieh, T.-M. Antibacterial TaN-Ag Coatings on Titanium Dental Implants. *Surf. Coat. Technol.* **2010**, *205*, 1636–1641.
139. Nam, K. Y. *In Vitro* Antimicrobial Effect of the Tissue Conditioner Containing Silver Nanoparticles. *J. Adv. Prosthodont.* **2011**, *3*, 20–24.
140. Travan, A.; Marsich, E.; Donati, I.; Benincasa, M.; Giazzon, M.; Felisari, L.; Paoletti, S. Silver-Polysaccharide Nanocomposite Antimicrobial Coatings for Methacrylic Thermosets. *Acta Biomater.* **2011**, *7*, 337–346.
141. Elsaka, S. E.; Hamouda, I. M.; Swain, M. V. Titanium Dioxide Nanoparticles Addition to a Conventional Glass-Ionomer Restorative: Influence on Physical and Antibacterial Properties. *J. Dent.* **2011**, *39*, 589–598.
142. Kishen, A.; Shi, Z.; Shrestha, A.; Neoh, K. G. An Investigation on the Antibacterial and Antibiofilm Efficacy of Cationic Nanoparticulates for Root Canal Disinfection. *J. Endod.* **2008**, *34*, 1515–1520.
143. Aydin Sevinc, B.; Hanley, L. Antibacterial Activity of Dental Composites Containing Zinc Oxide Nanoparticles. *J. Biomed. Mater. Res. B* **2010**, *94*, 22–31.
144. Tayel, A. A.; El-Tras, W. F.; Moussa, S.; El-Baz, A. F.; Mahrous, H.; Salem, M. F.; Brimer, L. Antibacterial Action of Zinc Oxide Nanoparticles Against Foodborne Pathogens. *J. Food Safety* **2011**, *31*, 211–218.
145. Ren, G.; Hu, D.; Cheng, E. W.; Vargas-Reus, M. A.; Reip, P.; Allaker, R. P. Characterisation of Copper Oxide Nanoparticles for Antimicrobial Applications. *Int. J. Antimicrob. Agents* **2009**, *33*, 587–590.
146. Morones, J. R.; Elechiguerra, J. L.; Camacho, A.; Holt, K.; Kouri, J. B.; Ramirez, J. T.; Yacaman, M. J. The Bactericidal Effect of Silver Nanoparticles. *Nanotechnology* **2005**, *16*, 2346–2353.
147. Verran, J.; Sandoval, G.; Allen, N. S.; Edge, M.; Stratton, J. Variables Affecting the Antibacterial Properties of Nano and Pigmentary Titania Particles in Suspension. *Dyes Pigments* **2007**, *73*, 298–304.
148. Pal, S.; Tak, Y. K.; Song, J. M. Does the Antibacterial Activity of Silver Nanoparticles Depend on the Shape of the Nanoparticle? A Study of the Gram-Negative Bacterium *Escherichia coli*. *Appl. Environ. Microbiol.* **2007**, *73*, 1712–1720.
149. Suwanboon, S.; Amornpitoksuk, P.; Bangrak, P.; Sukolrat, A.; Muensit, N. The Dependence of Optical Properties on the Morphology and Defects of Nanocrystalline ZnO Powders and Their Antibacterial Activity. *J. Ceram. Process. Res.* **2010**, *11*, 547–551.
150. Mortazavi, V.; Nahrkhalaji, M. M.; Fathi, M. H.; Mousavi, S. B.; Esfahani, B. N. Antibacterial Effects of Sol-Gel-Derived Bioactive Glass Nanoparticle on Aerobic Bacteria. *J. Biomed. Mater. Res., Part A* **2010**, *94*, 160–168.
151. Beyth, N.; Yudovin-Farber, I.; Perez-Davidi, M.; Domb, A. J.; Weiss, E. I. Polyethyleneimine Nanoparticles Incorporated into Resin Composite Cause Cell Death and Trigger Biofilm Stress *in Vivo*. *Proc. Natl. Acad. Sci. U.S.A.* **2010**, *107*, 22038–22043.
152. Shvero, D. K.; Davidi, M. P.; Weiss, E. I.; Srerer, N.; Beyth, N. Antibacterial Effect of Polyethyleneimine Nanoparticles Incorporated in Provisional Cements Against *Streptococcus Mutans*. *J. Biomed. Mater. Res. B* **2010**, *94*, 367–371.
153. Cousins, B. G.; Allison, H. E.; Doherty, P. J.; Edwards, C.; Garvey, M. J.; Martin, D. S.; Williams, R. L. Effects of a Nanoparticulate Silica Substrate on Cell Attachment of *Candida Albicans*. *J. Appl. Microbiol.* **2007**, *102*, 757–765.
154. Gaikwad, R. M.; Sokolov, I. Silica Nanoparticles to Polish Tooth Surfaces for Caries Prevention. *J. Dent. Res.* **2008**, *87*, 980–983.
155. Ruparelia, J. P.; Chatterjee, A. K.; Duttagupta, S. P.; Mukherji, S. Strain Specificity in Antimicrobial Activity

of Silver and Copper Nanoparticles. *Acta Biomater.* **2008**, *4*, 707–716.
156. Llorens, A.; Lloret, E.; Picouet, P. A.; Trbojevich, R.; Fernandez, A. Metallic-Based Micro and Nanocomposites in Food Contact Materials and Active Food Packaging. *Trends Food Sci. Technol.* **2012**, *24*, 19–29.
157. Vidic, J.; Stankic, S.; Haque, F.; Ciric, D.; Goffic, R.; Vidy, A.; Jupille, J.; Delmas, B. Selective Antibacterial Effects of Mixed ZnMgO Nanoparticles. *J. Nanopart. Res.* **2013**, *15*, 1–10.
158. Juillerat-Jeanneret, L.; Dusinska, M.; Fjellsbo, L. M.; Collins, A. R.; Handy, R. D.; Riediker, M. Biological Impact Assessment of Nanomaterial Used in Nanomedicine. Introduction to the NanoTEST Project. *Nanotoxicology* **2013**, *16*, 16.
159. Hook, E. R.; Owen, O. J.; Bellis, C. A.; Holder, J. A.; O'Sullivan, D. J.; Barbour, M. E. Development of a Novel Antimicrobial-Releasing Glass Ionomer Cement Functionalized with Chlorhexidine Hexametaphosphate Nanoparticles. *J. Nanobiotechnology* **2014**, *12*, 3.
160. Imazato, S.; Torii, M.; Tsuchitani, Y.; McCabe, J. F.; Russell, R. R. Incorporation of Bacterial Inhibitor into Resin Composite. *J. Dent. Res.* **1994**, *73*, 1437–1443.
161. Cramer, N. B.; Stansbury, J. W.; Bowman, C. N. Recent Advances and Developments in Composite Dental Restorative Materials. *J. Dent. Res.* **2011**, *90*, 402–416.
162. Chen, M. H. Update on Dental Nanocomposites. *J. Dent. Res.* **2010**, *89*, 549–560.
163. Hervas-Garcia, A.; Martinez-Lozano, M. A.; Cabanes-Vila, J.; Barjau-Escribano, A.; Fos-Galve, P. Composite Resins. A Review of the Materials and Clinical Indications. *Med. Oral Patol. Oral* **2006**, *11*, 215–220.
164. Lutz, F.; Phillips, R. W. A Classification and Evaluation of Composite Resin Systems. *J. Prosthet. Dent.* **1983**, *50*, 480–488.
165. Lang, B. R.; Jaarda, M.; Wang, R. F. Filler Particle Size and Composite Resin Classification Systems. *J. Oral Rehabil.* **1992**, *19*, 569–584.
166. Terry, D. A. Applications of Nanotechnology. *Pract. Proced. Aesthet. Dent.* **2004**, *16*, 220–222.
167. Mota, E. G.; Oshima, H. M.; Burnett, L. H., Jr.; Pires, L. A.; Rosa, R. S. Evaluation of Diametral Tensile Strength and Knoop Microhardness of Five Nanofilled Composites in Dentin and Enamel Shades. *Stomatologija* **2006**, *8*, 67–69.
168. Lohbauer, U.; Wagner, A.; Belli, R.; Stoetzel, C.; Hilpert, A.; Kurland, H. D.; Grabow, J.; Muller, F. A. Zirconia Nanoparticles Prepared by Laser Vaporization As Fillers for Dental Adhesives. *Acta Biomater.* **2010**, *6*, 4539–4546.
169. Atai, M.; Solhi, L.; Nodehi, A.; Mirabedini, S. M.; Kasraei, S.; Akbari, K.; Babanzadeh, S. PMMA-Grafted Nanoclay As Novel filler for Dental Adhesives. *Dent. Mater.* **2009**, *25*, 339–347.
170. Xu, H. H.; Moreau, J. L.; Sun, L.; Chow, L. C. Novel CaF(2) Nanocomposite with High Strength and Fluoride Ion Release. *J. Dent. Res.* **2010**, *89*, 739–745.
171. Sadat-Shojai, M.; Atai, M.; Nodehi, A.; Khanlar, L. N. Hydroxyapatite Nanorods As Novel Fillers for Improving the Properties of Dental Adhesives: Synthesis and Application. *Dent. Mater.* **2010**, *26*, 471–482.
172. Hosseinalipour, M.; Javadpour, J.; Rezaie, H.; Dadras, T.; Hayati, A. N. Investigation of Mechanical Properties of Experimental Bis-GMA/TEGDMA Dental Composite Resins Containing Various Mass Fractions of Silica Nanoparticles. *J. Prosthodont.* **2010**, *19*, 112–117.
173. Prentice, L. H.; Tyas, M. J.; Burrow, M. F. The Effect of Ytterbium Fluoride and Barium Sulphate Nanoparticles on the Reactivity and Strength of a Glass-Ionomer Cement. *Dent. Mater.* **2006**, *22*, 746–751.
174. Ruttermann, S.; Wandrey, C.; Raab, W. H.; Janda, R. Novel Nano-Particles As Fillers for an Experimental Resin-Based Restorative Material. *Acta Biomater.* **2008**, *4*, 1846–1853.
175. Zhang, F.; Xia, Y.; Xu, L.; Gu, N. Surface Modification and Microstructure of Single-Walled Carbon Nanotubes for Dental Resin-Based Composites. *J. Biomed. Mater. Res. B* **2008**, *86*, 90–97.
176. Ma, P.-C.; Siddiqui, N. A.; Marom, G.; Kim, J.-K. Dispersion and Functionalization of Carbon Nanotubes for Polymer-Based Nanocomposites: A Review. *Composites, Part A* **2010**, *41*, 1345–1367.
177. Kim, J. J.; Moon, H. J.; Lim, B. S.; Lee, Y. K.; Rhee, S. H.; Yang, H. C. The Effect of Nanofiller on the Opacity of Experimental Composites. *J. Biomed. Mater. Res. B* **2007**, *80*, 332–338.
178. Schulz, H.; Schimmoeller, B.; Pratsinis, S. E.; Salz, U.; Bock, T. Radiopaque Dental Adhesives: Dispersion of Flame-Made Ta2O5/SiO2 Nanoparticles in Methacrylic Matrices. *J. Dent.* **2008**, *36*, 579–587.
179. Moy, P. K.; Medina, D.; Shetty, V.; Aghaloo, T. L. Dental Implant Failure Rates and Associated Risk Factors. *Int. J. Oral Maxillofac. Implants* **2005**, *20*, 569–577.
180. Salata, O. Applications of Nanoparticles in Biology and Medicine. *J. Nanobiotechnol.* **2004**, *2*, 3.
181. Silva, G. A. Introduction to Nanotechnology and Its Applications to Medicine. *Surg. Neurol.* **2004**, *61*, 216–220.
182. Meirelles, L.; Arvidsson, A.; Andersson, M.; Kjellin, P.; Albrektsson, T.; Wennerberg, A. Nano Hydroxyapatite Structures Influence Early Bone Formation. *J. Biomed. Mater. Res., Part A* **2008**, *87*, 299–307.
183. Bertazzo, S.; Zambuzzi, W. F.; Campos, D. D.; Ferreira, C. V.; Bertran, C. A. A Simple Method for Enhancing Cell Adhesion to Hydroxyapatite Surface. *Clin. Oral Implants Res.* **2010**, *21*, 1411–1413.
184. Hayami, T.; Hontsu, S.; Higuchi, Y.; Nishikawa, H.; Kusunoki, M. Osteoconduction of a Stoichiometric and Bovine Hydroxyapatite Bilayer-Coated Implant. *Clin. Oral Implants Res.* **2011**, *22*, 774–776.
185. Mistry, S.; Kundu, D.; Datta, S.; Basu, D. Comparison of Bioactive Glass Coated and Hydroxyapatite Coated Titanium Dental Implants in the Human Jaw Bone. *Aust. Dent. J.* **2011**, *56*, 68–75.
186. Quaranta, A.; Iezzi, G.; Scarano, A.; Coelho, P. G.; Vozza, I.; Marincola, M.; Piattelli, A. A Histomorphometric Study of Nanothickness and Plasma-Sprayed Calcium-Phosphorous-Coated Implant Surfaces in Rabbit Bone. *J. Periodontol.* **2010**, *81*, 556–561.
187. Hamlet, S.; Ivanovski, S. Inflammatory Cytokine Response to Titanium Chemical Composition and Nanoscale Calcium Phosphate Surface Modification. *Acta Biomater.* **2011**, *7*, 2345–2353.
188. Lin, A.; Wang, C. J.; Kelly, J.; Gubbi, P.; Nishimura, I. The Role of Titanium Implant Surface Modification with Hydroxyapatite Nanoparticles in Progressive Early Bone-Implant Fixation *in Vivo*. *Int. J. Oral Maxillofac. Implants* **2009**, *24*, 808–816.
189. Yang, G. L.; He, F. M.; Hu, J. A.; Wang, X. X.; Zhao, S. F. Effects of Biomimetically and Electrochemically Deposited Nano-Hydroxyapatite Coatings on Osseointegration of Porous Titanium Implants. *Oral Surg., Oral Med., Oral Pathol.* **2009**, *107*, 782–789.
190. He, F.; Yang, G.; Wang, X.; Zhao, S. Effect of Electrochemically Deposited Nanohydroxyapatite on Bone Bonding of Sandblasted/Dual Acid-Etched Titanium Implant. *Int. J. Oral Maxillofac. Implants* **2009**, *24*, 790–799.
191. Svanborg, L. M.; Hoffman, M.; Andersson, M.; Currie, F.; Kjellin, P.; Wennerberg, A. The Effect of Hydroxyapatite Nanocrystals on Early Bone Formation Surrounding Dental Implants. *Int. J. Oral Maxillofac. Surg.* **2011**, *40*, 308–315.
192. Mankani, M. H.; Kuznetsov, S. A.; Fowler, B.; Kingman, A.; Robey, P. G. *In Vivo* Bone Formation by Human Bone Marrow Stromal Cells: Effect of Carrier Particle Size and Shape. *Biotechnol. Bioeng.* **2001**, *72*, 96–107.
193. Shi, Z.; Huang, X.; Cai, Y.; Tang, R.; Yang, D. Size Effect of Hydroxyapatite Nanoparticles on Proliferation and Apoptosis of Osteoblast-Like Cells. *Acta Biomater.* **2009**, *5*, 338–345.
194. Goene, R. J.; Testori, T.; Trisi, P. Influence of a Nanometer-Scale Surface Enhancement on *de Novo* Bone Formation on Titanium Implants: A Histomorphometric Study in

Human Maxillae. *Int. J. Periodont. Restor. Dent.* **2007**, *27*, 211–219.
195. Telleman, G.; Albrektsson, T.; Hoffman, M.; Johansson, C. B.; Vissink, A.; Meijer, H. J.; Raghoebar, G. M. Peri-Implant Endosseous Healing Properties of Dual Acid-Etched Mini-Implants with a Nanometer-Sized Deposition of CaP: A Histological and Histomorphometric Human Study. *Clin. Implant Dent. Relat. Res.* **2010**, *12*, 153–160.
196. Bucci-Sabattini, V.; Cassinelli, C.; Coelho, P. G.; Minnici, A.; Trani, A.; Dohan Ehrenfest, D. M. Effect of Titanium Implant Surface Nanoroughness and Calcium Phosphate Low Impregnation on Bone Cell Activity *in Vitro*. *Oral Surg., Oral Med., Oral Pathol.* **2010**, *109*, 217–224.
197. Webster, T. J.; Ergun, C.; Doremus, R. H.; Siegel, R. W.; Bizios, R. Enhanced Functions of Osteoblasts on Nanophase Ceramics. *Biomaterials* **2000**, *21*, 1803–1810.
198. Webster, T. J.; Hellenmeyer, E. L.; Price, R. L. Increased Osteoblast Functions on Theta + Delta Nanofiber Alumina. *Biomaterials* **2005**, *26*, 953–960.
199. Yang, L.; Sheldon, B. W.; Webster, T. J. Orthopedic Nano Diamond Coatings: Control of Surface Properties and Their Impact on Osteoblast Adhesion and Proliferation. *J. Biomed. Mater. Res., Part A* **2009**, *91*, 548–556.
200. Radice, S.; Kern, P.; Burki, G.; Michler, J.; Textor, M. Electrophoretic Deposition of Zirconia-Bioglass Composite Coatings for Biomedical Implants. *J. Biomed. Mater. Res., Part A* **2007**, *82*, 436–444.
201. Coelho, P. G.; Cardaropoli, G.; Suzuki, M.; Lemons, J. E. Early Healing of Nanothickness Bioceramic Coatings on Dental Implants. An Experimental Study in Dogs. *J. Biomed. Mater. Res. B* **2009**, *88*, 387–393.
202. Schouten, C.; Meijer, G. J.; van den Beucken, J. J.; Leeuwenburgh, S. C.; de Jonge, L. T.; Wolke, J. G.; Spauwen, P. H.; Jansen, J. A. *In Vivo* Bone Response and Mechanical Evaluation of Electrosprayed CaP Nanoparticle Coatings Using the Iliac Crest of Goats As an Implantation Model. *Acta Biomater.* **2010**, *6*, 2227–2236.
203. Al-Hamdan, K.; Al-Moaber, S. H.; Junker, R.; Jansen, J. A. Effect of Implant Surface Properties on Peri-Implant Bone Healing: A Histological and Histomorphometric Study in Dogs. *Clin. Oral Implants Res.* **2011**, *22*, 399–405.
204. Mendes, V. C.; Moineddin, R.; Davies, J. E. The Effect of Discrete Calcium Phosphate Nanocrystals on Bone-Bonding to Titanium Surfaces. *Biomaterials* **2007**, *28*, 4748–4755.
205. Wennerberg, A.; Albrektsson, T. Effects of Titanium Surface Topography on Bone Integration: A Systematic Review. *Clin. Oral Implants Res.* **2009**, *20*, 172–184.
206. Loberg, J.; Mattinson, I.; Hansson, S.; Ahlberg, E. Characterisation of Titanium Dental Implants I: Critical Assessment of Surface Roughness Parameters. *Open Biomater. J.* **2010**, *2*, 18–35.
207. Breding, K.; Jimbo, R.; Hayashi, M.; Xue, Y.; Mustafa, K.; Andersson, M. The Effect of Hydroxyapatite Nanocrystals on Osseointegration of Titanium Implants: an *in Vivo* Rabbit Study. *Int. J. Dent.* **2014**, *171305*, 9.
208. Jeong, S. H.; Jang, S. O.; Kim, K. N.; Kwon, H. K.; Park, Y. D.; Kim, B. I. Remineralization Potential of New Toothpaste Containing Nano-Hydroxyapatite. *Key Eng. Mater.* **2006**, *309−311*, 537–540.
209. Lu, K. L.; Zhang, J. X.; Meng, X. C.; Wei, G. Z.; Zhou, M. L. Effects of Nano-Hydroxyapatite on the Artificial Caries. *Mater. Sci. Technol.* **2006**, *14*, 633–636.
210. Lv, K. L.; Zhang, J. X.; Meng, X. C.; Li, X. Y. Remineralization Effect of the Nano-HA Toothpaste on Artificial Caries. *Key Eng. Mater.* **2007**, *330−332*, 267–270.
211. Tschoppe, P.; Zandim, D. L.; Martus, P.; Kielbassa, A. M. Enamel and Dentine Remineralization by Nano-Hydroxyapatite Toothpastes. *J. Dent.* **2011**, *39*, 430–437.
212. Forsback, A. P.; Areva, S.; Salonen, J. I. Mineralization of Dentin Induced by Treatment with Bioactive Glass S53P4 *in Vitro*. *Acta Odontol. Scand.* **2004**, *62*, 14–20.
213. Vollenweider, M.; Brunner, T. J.; Knecht, S.; Grass, R. N.; Zehnder, M.; Imfeld, T.; Stark, W. J. Remineralization of Human Dentin Using Ultrafine Bioactive Glass Particles. *Acta Biomater.* **2007**, *3*, 936–943.
214. Jeong, S. H.; Hong, S. J.; Choi, C. H.; Kim, B. I. Effect of New Dentifrice Containing Nano-Sized Carbonated Apatite on Enamel Remineralization. *Key Eng. Mater.* **2007**, *330−332*, 291–294.
215. Nakashima, S.; Yoshie, M.; Sano, H.; Bahar, A. Effect of a Test Dentifrice Containing Nano-Sized Calcium Carbonate on Remineralization of Enamel Lesions *in Vitro*. *J. Oral Sci.* **2009**, *51*, 69–77.
216. Sun, L. M.; Chow, L. C. Preparation and Properties of Nano-Sized Calcium Fluoride for Dental Applications. *Dent. Mater.* **2008**, *24*, 111–116.
217. Roveri, N.; Battistella, E.; Foltran, I.; Foresti, E.; Iafisco, M.; Lelli, M.; Palazzo, B.; Rimondini, L. Synthetic Biomimetic Carbonate-Hydroxyapatite Nanocrystals for Enamel Remineralization. *Adv. Mater. Res.* **2008**, *47−50*, 821–824.
218. Reynolds, E. C. Anticariogenic Complexes of Amorphous Calcium Phosphate Stabilized by Casein Phosphopeptides: A Review. *Spec. Care Dentist* **1998**, *18*, 8–16.
219. Chiang, Y. C.; Chen, H. J.; Liu, H. C.; Kang, S. H.; Lee, B. S.; Lin, F. H.; Lin, H. P.; Lin, C. P. A Novel Mesoporous Biomaterial for Treating Dentin Hypersensitivity. *J. Dent. Res.* **2010**, *89*, 236–240.
220. Markowitz, K. The Original Desensitizers: Strontium and Potassium Salts. *J. Clin. Dent.* **2009**, *20*, 145–151.
221. Uchida, A.; Wakano, Y.; Fukuyama, O.; Miki, T.; Iwayama, Y.; Okada, H. Controlled Clinical Evaluation of a 10% Strontium Chloride Dentifrice in Treatment of Dentin Hypersensitivity Following Periodontal Surgery. *J. Periodontol.* **1980**, *51*, 578–581.
222. Minkoff, S.; Axelrod, S. Efficacy of Strontium Chloride in Dental Hypersensitivity. *J. Periodontol.* **1987**, *58*, 470–474.
223. Dabas, V. K.; Swadia, U. H. Comparative Study of Effectiveness of Strontium Chloride and Formalin Containing Dentifrices in Relieving Dental Hypersensitivity. *Indian J. Dent. Res.* **1989**, *1*, 15–21.
224. Zappa, U. Self-Applied Treatments in the Management of Dentine Hypersensitivity. *Arch. Oral Biol.* **1994**, *39*, 107–112.
225. Cummins, D. Recent Advances in Dentin Hypersensitivity: Clinically Proven Treatments for Instant and Lasting Sensitivity Relief. *Am. J. Dent.* **2010**, *23*, 3–13.
226. Kleinberg, I. SensiStat. A New Saliva-Based Composition for Simple and Effective Treatment of Dentinal Sensitivity Pain. *Dent. Today* **2002**, *21*, 42–47.
227. Cummins, D. The Efficacy of a New Dentifrice Containing 8.0% Arginine, Calcium Carbonate, and 1450 ppm Fluoride in Delivering Instant and Lasting Relief of Dentin Hypersensitivity. *J. Clin. Dent.* **2009**, *20*, 109–114.
228. Kodaka, T.; Kuroiwa, M.; Okumura, J.; Mori, R.; Hirasawa, S.; Kobori, M. Effects of Brushing with a Dentifrice for Sensitive Teeth on Tubule Occlusion and Abrasion of Dentin. *J. Electron. Microsc.* **2001**, *50*, 57–64.
229. Schulte, P. A.; Geraci, C. L.; Murashov, V.; Kuempel, E. D.; Zumwalde, R. D.; Castranova, V.; Hoover, M. D.; Hodson, L.; Martinez, K. F. Occupational Safety and Health Criteria for Responsible Development of Nanotechnology. *J. Nanopart. Res.* **2014**, *16*, 2153.
230. Jani, P. U.; McCarthy, D. E.; Florence, A. T. Titanium Dioxide (Rutile) Particle Uptake from the Rat GI Tract and Translocation to Systemic Organs after Oral Administration. *Int. J. Pharm.* **1994**, *105*, 157–168.
231. Wang, J.; Zhou, G.; Chen, C.; Yu, H.; Wang, T.; Ma, Y.; Jia, G.; Gao, Y.; Li, B.; Sun, J.; et al. Acute Toxicity and Biodistribution of Different Sized Titanium Dioxide Particles in Mice after Oral Administration. *Toxicol. Lett.* **2007**, *168*, 176–185.
232. Chen, Z.; Meng, H.; Xing, G.; Chen, C.; Zhao, Y.; Jia, G.; Wang, T.; Yuan, H.; Ye, C.; Zhao, F.; et al. Acute Toxicological Effects of Copper Nanoparticles *in Vivo*. *Toxicol. Lett.* **2006**, *163*, 109–120.
233. Ramsden, C. S.; Smith, T. J.; Shaw, B. J.; Handy, R. D. Dietary Exposure to Titanium Dioxide Nanoparticles in Rainbow Trout, (*Oncorhynchus Mykiss*): No Effect on Growth, but Subtle Biochemical Disturbances in the Brain. *Ecotoxicology* **2009**, *18*, 939–951.

234. Fraser, T. W.; Reinardy, H. C.; Shaw, B. J.; Henry, T. B.; Handy, R. D. Dietary Toxicity of Single-Walled Carbon Nanotubes and Fullerenes (C60) in Rainbow Trout (*Oncorhynchus Mykiss*). *Nanotoxicology* **2011**, *5*, 98–108.
235. Koeneman, B. A.; Zhang, Y.; Westerhoff, P.; Chen, Y.; Crittenden, J. C.; Capco, D. G. Toxicity and Cellular Responses of Intestinal Cells Exposed to Titanium Dioxide. *Cell Biol. Toxicol.* **2010**, *26*, 225–238.
236. Gitrowski, C.; Al-Jubory, A. R.; Handy, R. D. Uptake of Different Crystal Structures of TiO2 Nanoparticles by Caco-2 Intestinal Cells. *Toxicol. Lett.* **2014**, *226*, 264–276.
237. Chung, I. S.; Lee, M. Y.; Shin, D. H.; Jung, H. R. Three Systemic Argyria Cases after Ingestion of Colloidal Silver Solution. *Int. J. Dermatol.* **2010**, *49*, 1175–1177.
238. Bouwmeester, H.; Dekkers, S.; Noordam, M. Y.; Hagens, W. I.; Bulder, A. S.; de Heer, C.; ten Voorde, S. E.; Wijnhoven, S. W.; Marvin, H. J.; Sips, A. J. Review of Health Safety Aspects of Nanotechnologies in Food Production. *Regul. Toxicol. Pharmacol.* **2009**, *53*, 52–62.
239. Brune, D. Metal Release from Dental Biomaterials. *Biomaterials* **1986**, *7*, 163–175.
240. Gerzina, T. M.; Hume, W. R. Effect of Dentine on Release of TEGDMA from Resin Composite *in Vitro*. *J. Oral Rehabil.* **1994**, *21*, 463–468.
241. Ferracane, J. L. Elution of Leachable Components from Composites. *J. Oral Rehabil.* **1994**, *21*, 441–452.
242. Olea, N.; Pulgar, R.; Perez, P.; Olea-Serrano, F.; Rivas, A.; Novillo-Fertrell, A.; Pedraza, V.; Soto, A. M.; Sonnenschein, C. Estrogenicity of Resin-Based Composites and Sealants Used in Dentistry. *Environ. Health Perspect.* **1996**, *104*, 298–305.
243. Geurtsen, W. Biocompatibility of Root Canal Filling Materials. *Aust. Endod. J.* **2001**, *27*, 12–21.
244. Collins, L. M.; Dawes, C. The Surface Area of the Adult Human Mouth and Thickness of the Salivary Film Covering the Teeth and Oral Mucosa. *J. Dent. Res.* **1987**, *66*, 1300–1302.
245. Harris, D.; Robinson, J. R. Drug Delivery *via* the Mucous Membranes of the Oral Cavity. *J. Pharm. Sci.* **1992**, *81*, 1–10.
246. Takubo, K. *Pathology of the Esophageus: An Atlas and Textbook*, second ed.; Springer Verlag: Tokyo, 2009; p 363.
247. Atuma, C.; Strugala, V.; Allen, A.; Holm, L. The Adherent Gastrointestinal Mucus Gel Layer: Thickness and Physical State *in Vivo*. *Am. J. Physiol-Gastr. L.* **2001**, *280*, 922–929.
248. Handy, R. D.; Henry, T. B.; Scown, T. M.; Johnston, B. D.; Tyler, C. R. Manufactured Nanoparticles: Their Uptake and Effects on Fish - A Mechanistic Analysis. *Ecotoxicology* **2008**, *17*, 396–409.
249. Lai, S. K.; Wang, Y. Y.; Hanes, J. Mucus-Penetrating Nanoparticles for Drug and Gene Delivery to Mucosal Tissues. *Adv. Drug Delivery Rev.* **2009**, *61*, 158–171.
250. Dobrovolskaia, M. A.; McNeil, S. E. Immunological Properties of Engineered Nanomaterials. *Nat. Nanotechnol.* **2007**, *2*, 469–478.
251. Hunt, G.; Lynch, I.; Cassee, F.; Handy, R. D.; Fernandes, T. F.; Berges, M.; Kuhlbusch, T. A. J.; Dusinska, M.; Riediker, M. Towards a Consensus View on Understanding Nanomaterials Hazards and Managing Exposure: Knowledge Gaps and Recommendations. *Materials* **2013**, *6*, 1090–1117.
252. Engeman, C. D.; Baumgartner, L.; Carr, B. M.; Fish, A. M.; Meyerhofer, J. D.; Satterfield, T. A.; Holden, P. A.; Harthorn, B. H. Governance Implications of Nanomaterials Companies' Inconsistent Risk Perceptions and Safety Practices. *J. Nanopart. Res.* **2012**, *14*, 749–761.
253. Berges, M. G. M. Exposure During Production and Handling of Manufactured Nanomaterials. In *Nanomaterials*. Commission for the Investigation of Health Hazards of Chemical Compounds in the Work Area. Report by Deutsche Forschungsgemeinschaft (German Research Foundation); Wiley-VCH: Berlin, Germany, 2013; pp 25−31.
254. Kuhlbusch, T. A.; Asbach, C.; Fissan, H.; Gohler, D.; Stintz, M. Nanoparticle Exposure at Nanotechnology Workplaces: A Review. *Part. Fibre Toxicol.* **2011**, *8*, 22.
255. Shrestha, A.; Hamblin, M. R.; Kishen, A. Photoactivated Rose Bengal Functionalized Chitosan Nanoparticles Produce Antibacterial/Biofilm Activity and Stabilize Dentin-Collagen. *Nanomed.-Nanotechnol.* **2014**, *10*, 491–501.
256. Kasraei, S.; Sami, L.; Hendi, S.; Alikhani, M. Y.; Rezaei-Soufi, L.; Khamverdi, Z. Antibacterial Properties of Composite Resins Incorporating Silver and Zinc Oxide Nanoparticles on *Streptococcus Mutans* and *Lactobacillus*. *Restor. Dent. Endod.* **2014**, *39*, 109–14.
257. Cheng, L.; Weir, M. D.; Zhang, K.; Arola, D. D.; Zhou, X.; Xu, H. H. K. Dental Primer and Adhesive Containing a New Antibacterial Quaternary Ammonium Monomer Dimethylaminododecyl Methacrylate. *J. Dent.* **2013**, *41*, 345–355.
258. Waltimo, T.; Mohn, D.; Paque, F.; Brunner, T. J.; Stark, W. J.; Imfeld, T.; Schatzle, M.; Zehnder, M. Fine-Tuning of Bioactive Glass for Root Canal Disinfection. *J. Dent. Res.* **2009**, *88*, 235–238.
259. Canche-Escamilla, G.; Duarte-Aranda, S.; Toledano, M. Synthesis and Characterization of Hybrid Silica/PMMA Nanoparticles and Their Use As Filler in Dental Composites. *Mater. Sci. Eng. C: Mater. Biol. Appl.* **2014**, *42*, 161–167.
260. Wagner, A.; Belli, R.; Stötzel, C.; Hilpert, A.; Müller, F. A.; Lohbauer, U. Biomimetically- and Hydrothermally-Grown HAp Nanoparticles as Reinforcing Fillers for Dental Adhesives. *J. Adhes. Dent.* **2013**, *15*, 413–422.
261. Sasani, N.; Vahdati Khaki, J.; Mojtaba Zebarjad, S. Characterization and Nanomechanical Properties of Novel Dental Implant Coatings Ccontaining Copper Decorated-Carbon Nanotubes. *J. Mech. Behav. Biomed.* **2014**, *37*, 125–132.
262. Shi, J.; Dong, L. L.; He, F.; Zhao, S.; Yang, G.-L. Osteoblast Responses to Thin Nanohydroxyapatite Coated on Roughened Titanium Surfaces Deposited by an Electrochemical Process. *Oral Surg., Oral Med., Oral Pathol.* **2013**, *116*, 311–316.
263. Lee, H.-H.; Sang Shin, U.; Lee, J.-H.; Kim, H.-W. Biomedical Nanocomposites of Poly(Lactic Acid) and Calcium Phosphate Hybridized with Modified Carbon Nanotubes for Hard Tissue Implants. *J. Biomed. Mater. Res. B* **2011**, *98B*, 246–254.
264. Dabbagh, A.; Abu Kasim, N. H.; Bakri, M. M.; Wakily, H.; Ramasindarum, C.; Abdullah, B. J. J. Polyethylene-Glycol Coated Maghemite Nanoparticles for Treatment of Dental Hypersensitivity. *Mater. Lett.* **2014**, *121*, 89–92.
265. Shrivastava, R.; Kushwaha, P.; Bhutia, Y. C.; Flora, S. Oxidative Stress Induced Following Exposure to Silver and Gold Nanoparticles in Mice. *Toxicol. Ind. Health* **2014**, 1–14.
266. Yang, K.; Gong, H.; Shi, X.; Wan, J.; Zhang, Y.; Liu, Z. *In Vivo* Biodistribution and Toxicology of Functionalized Nano-Graphene Oxide in Mice After Oral and Intraperitoneal Administration. *Biomaterials* **2013**, *34*, 2787–2795.
267. Greish, K.; Thiagarajan, G.; Herd, H.; Price, R.; Bauer, H.; Hubbard, D.; Burckle, A.; Sadekar, S.; Yu, T.; Anwar, A.; et al. Size and Surface Charge Significantly Influence the Toxicity of Silica and Dendritic Nanoparticles. *Nanotoxicology* **2012**, *6*, 713–723.
268. Prabhakar, P. V.; Reddy, U. A.; Singh, S. P.; Balasubramanyam, A.; Rahman, M. F.; Indu Kumari, S.; Agawane, S. B.; Murty, U. S.; Grover, P.; Mahboob, M. Oxidative Stress Induced by Aluminum Oxide Nanomaterials after Acute Oral Treatment in Wistar rats. *J. Appl. Toxicol.* **2012**, *32*, 436–445.
269. Zhang, R.; Niu, Y.; Li, Y.; Zhao, C.; Song, B.; Zhou, Y. Acute Toxicity Study of the Interaction between Titanium Dioxide Nanoparticles and Lead Acetate in Mice. *Environ. Toxicol. Pharmacol.* **2010**, *30*, 52–60.
270. Trouiller, B.; Reliene, R.; Westbrook, A.; Solaimani, P.; Schiestl, R. H. Titanium Dioxide Nanoparticles Induce DNA Damage and Ggenetic Instability *in Vivo* in Mice. *Cancer Res.* **2009**, *69*, 8784–8789.